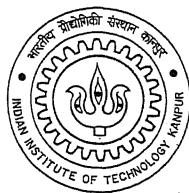


# STUDIES ON LASER RANGING SYSTEMS

A Thesis Submitted  
in Partial Fulfillment of the Requirements  
for the degree of  
Master of Technology

*by*

Valluri Sarimela



*to the*

DEPARTMENT OF ELECTRICAL ENGINEERING  
INDIAN INSTITUTE OF TECHNOLOGY  
KANPUR

11 MAY 2000/EE  
CENTRAL LIBRARY  
I. I. T., KANPUR

~~130806~~ A 130806

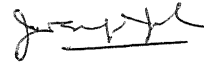
TH  
EE/2000/M  
Sa 738



A130806

## CERTIFICATE

It is certified that the work contained in the thesis entitled "**Studies On Laser Ranging Systems**", by Valluri Sarimela (Roll No.9810460), has been carried out under my supervision and this work has not been submitted elsewhere for a degree.



(JOSEPH JOHN)

10 March, 2000

Associate Professor

Dept. of Elect.Engg.

I.I.T. Kanpur 208016

*Dedicated*

*to*

Dr. Joseph John and his family

(My thesis supervisor, his wife Nina Joseph and their son

Timothy Joseph)

*For their unconditional love and support.*



## ACKNOWLEDGEMENTS

I am most indebted and grateful to my guide Dr. Joseph John for his encouragement and valuable guidance throughout my work. He is always very patient and cooperative to me while discussing the various aspects of the work. He is always available to me whenever I need inspite of his busy schedule. Without him it would have been impossible to conceive this.

I would like to thank his family, who opened their home for me. I am especially thankful to Nina-chechi who always encouraged me both spiritually and morally and supported me during my stay at the campus which was very pleasant.

I would like to thank Dr. V.N kulkarni's family they are always very kind and generous towards me. I found their home like my own and all my life I shall remain very grateful to them.

My sincere thanks to Dr. Sundar Manohar's family, Abraham Uncle's family, Shivprasad's family who are always very caring and affectionate to me.

I am very grateful to my friend N.V.Ramana who is always very gentle, patient and kind hearted, helping me always whenever I need. My sincere thanks to my friends Murali, Prabhakar, Ravi and Sankar and their good company.

I am thankful to my friends Maymole didi, Manjulatha, Alpana Dutta, for their good company and encouragement. I am very grateful to my friend Shalini Gupta who is very simple and good hearted helping me in typing my thesis work. My sincere thanks to Sanjay and Chaitanya.

My sincere thanks to my teacher G. Kondala Rao whose inspiration and encouragement bringing me to achieve this. My sincere thanks to my parents.

Valluri.Sarimela

## ABSTRACT

An extensive study of various laser range-finding techniques was carried out for both long range and short range applications making use of various types of laser sources. The relative merits and demerits of available laser sources were pointed out. System considerations of the major blocks of a laser range finder were studied. Modern signal processing techniques for improving the performance of range measurement at low power outputs are considered. Improvement of the SNR at low power levels by using Pulse integration or signal averaging technique is discussed. A digital signal averager scheme was designed and implemented using a high speed 8-bit ADC, RAM, and DAC. Timing and control-signal generators for the above averager were implemented using standard digital hardware. For typical receiver outputs, signal build up was observed on the CRO. Improvements to the above design are suggested. Simple transmitter and receiver circuit schemes were carried out and implemented.

## TABLE OF CONTENTS

Chapter 1:Introduction	1
1.1 System overview	1
1.2 Thesis objective	3
1.3 Thesis layout	4
Chapter 2:Laser Sources For Range Finding	5
2.1 Solid State Lasers	5
2.1.1 Q-Switching	6
2.1.2 Cavity Dumping	7
2.1.3 Mode locking	7
2.1.4 Types of Solid-State Lasers	8
2.2 Gas Lasers	9
2.2.1 Pulsed CO <sub>2</sub> Laser Sources	9
2.2.2 CW Gas Laser	10
2.3 Semiconductor Lasers	11
Chapter 3: Review of Laser Range Finders	12
3.1 Basic Principal of Long Range Measurement	12
3.2 Range Measurement Systems using GaAs Laser diodes	15
3.3 Range Measurement Systems using CO <sub>2</sub> Laser	17

3.4	Range Measurement Systems using Nd YAG Lasers	20
3.5	Short Range Measurement Systems	22
3.5.1	Interferometric Technique	22
3.5.2	Phaseshift Measurement Technique	23
3.5.3	Optical Triangulation Method	24
Chapter 4: System Considerations of Laser Range Finders		26
4.1	Atmospheric propagation	27
4.1.1	Attenuation	27
4.2	Targets	28
4.2.1	Speckle effects (Signal fluctuations)	29
4.3	Receivers	30
4.3.1	Optical design	30
4.3.2	Photo detectors	31
4.3.3	Noise Sources	31
4.4	Pulse Integration	33
4.5	Choice of Transmitter Waveform	33
4.5.1	Range Finders using Natural Targets: Pulsed Sources and Direct Detection	33
4.5.2	Lunar Range Finders using Retro-Reflectors, Pulsed Sources and Direct Detection	34

4.5.3	Surveying Instruments using Retro Reflectors, Modulated CW Sources and Direct Detection.	34
4.6	Hetrodyne Detection Systems	34
4.7	Laser Eye-Hazards	36
4.7.1	Eye-safe Systems	36
4.8	Signal Averaging Techniques	36
4.8.1	Band Width Reduction Technique	36
4.8.2	Averaging or Integration Technique	37

## Chapter 5: Hardware Implementation of Laser Range Finder Subsystems

5.1	Hardware Implementation of a Digital Signal Averager	41
5.1.1	System Timing and Control signal Generators	42
5.1.2	AD7574 ADC and ADDER	46
5.1.3	Storing of Added Data in Memory(RAM)	47
5.1.4	Conversion of Digital Data to Analog signal and Display	49
5.1.5	Selection of Address lines (Address Counter)	50
5.1.6	Controlling of No.of Scans (Scanning Counter)	51
5.2	Input Signal Generation	52
5.3	Clearing the RAM data	53
5.4	Hardware Implementation of Subsections (Transmitter and Reciver)	53

## Chapter 6: Discussion of Results, Conclusions and Suggestions

for Future Work 58

REFERENCES 60

# CHAPTER 1

## INTRODUCTION

In the past, terrestrial opto-electronic distance measurement in the kilometer range was only possible by marking the targets with reflector prisms or by increasing the optical power output far beyond the eye safety limits. This is not acceptable for many measurement tasks. This problem can be avoided by employing low power laser sources and modern signal processing techniques. Nowadays optical range finders compete with the microwave radars because of the tremendous improvements in present day technology in the optical field, manufacturing of various lasers sources, photodetectors and other optical equipment. These range finders are very accurate in measuring distances. At present the design of the laser range finder appears to be much simpler than the conventional microwave radar systems. These range finders have the added advantages of immunity to EMI, comparatively lower cost, small size and weight, and easier maintenance. Laser range finders can be used for both civilian and military applications. Many such systems can easily track the moving targets as well. Other advantages include low power consumption for battery operated systems and compatibility with remote and control data transfer systems.

### **1.1 SYSTEM OVER VIEW**

The basic laser range finder consists of mainly the laser transmitter, receiver and associated optics. Fig 1.1 shows a simple functional block diagram of a typical laser range finder.

There are several techniques available to measure the range of a target, viz. time of flight method (TOF), interferometry, and phase-shift method. TOF method is based on a simple principle. The target whose range  $R$  to be determined is given by  $R = (ct/2) + K_0$ , where  $c$  is the velocity of the light and  $t$  the time interval between the departure of light

pulse from the transmitter and its arrival at the receiver. The constant  $K_0$  is the sum of the systematic effects such as signal propagation delays, thyristor switch time etc.

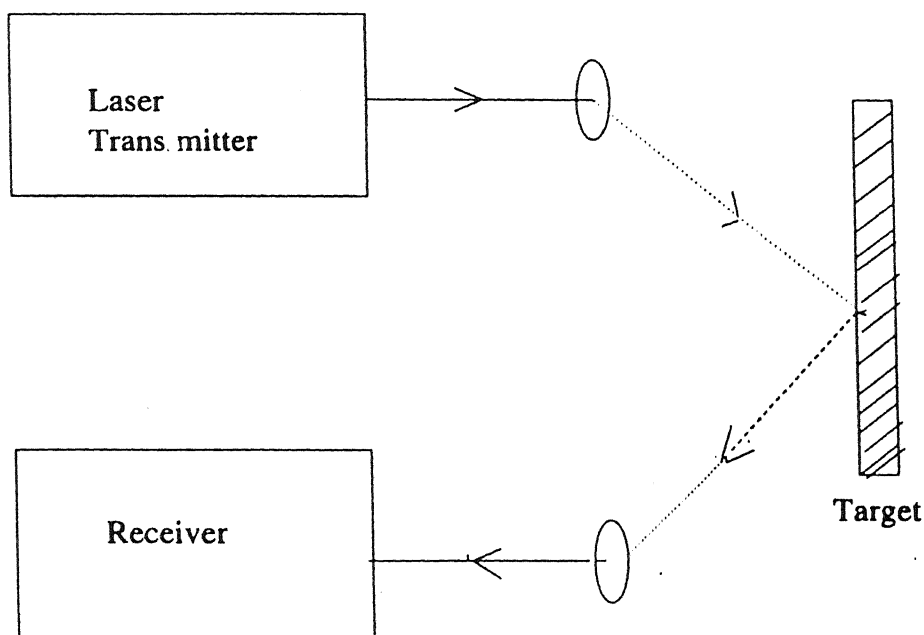


Fig1.1: Basic block diagram of laser range finder

**Transmitter:** There are several sources that are available to the designer, viz. Gas, solid state lasers, Nd:YAG, semiconductor lasers, and GaAs laser diodes. The choice of a particular laser source depends upon many parameters. Every source has its own advantages and disadvantages. The transmitter mainly consists of a light source and necessary drive and control circuitry. Increasingly, laser diodes are being used in range finding equipment. Because of their adequate output power, they are suitable for a wide range of applications, and their optical power is directly modulated by varying the input current to the device. The choice of a particular laser diode has to be made according to the required optical power output, beam quality, modulation frequency and depth, coherence length, etc.



**Receiver:** It comprises a photodetector, a preamplifier, post amplifier and signal restoring circuitry. The main function of the detector is to convert the optical signal into an electrical signal. It must meet very high performance requirements. The signal should be amplified with as minimum noise as possible so that it can be processed by subsequent signal processing stages to improve the signal-to-noise ratio. The echo signal from the target is often much weaker than the background radiation received from the sun. This background radiation however can be treated as a random noise and it can be suppressed by repetitive measurements. One such method is the pulse integration or the signal averaging technique. In this method the echo signal accumulates proportional to the number  $N$  of independent measurements while the noise increases as  $\sqrt{N}$ .

## **1.2 THESIS OBJECTIVE**

The main objective of the thesis is to study commonly used laser range finders and to design a suitable signal averager for an optical range finder. Improvements in range measurements are possible by implementing some modern signal processing techniques combined with low laser output power to meet eye safety requirements. Another critical limitation of the optical radar system is the background radiation. In most high power systems, threshold detection scheme is employed to overcome the background radiation. The principle of pulse integration is described and the hardware design of a digital signal averager is implemented. In this case after triggering the laser receiver, the signal is sampled and digitized at regular intervals, thus dividing the time axis into a series of windows or bins, each bin corresponding to a particular time interval. Distance is measured using the formula  $R = ct/2$ , where  $c$  is the velocity of light and  $t$  is the time of flight, between the exit of the laser pulse from the transmitter to the time the target signal is received. The width of the bin and nominal resolution depends on the speed of the ADC and rate at which the circuit can acquire and process the data. The incoming data is stored successive memory locations, thereby creating an image of the time axis. Each memory location contains one sample of the receiver signal in a particular time gate. Besides external physical limitations it is also the size of the available fast memory that limits the maximum range of the apparatus. By implementing a suitable signal averager the SNR can be improved.

### **1.3 THESIS LAYOUT**

The complete thesis is divided into six chapters. Chapter 1 gives an introduction to the thesis. A comprehensive review of different laser sources is given in Chapter 2. Different laser range finding techniques are reviewed in detail in Chapter 3, which discusses both long and short range measurements. In Chapter 4, system considerations of laser range finders are given. Chapter 5 gives the details of the digital signal averager which was implemented as a part of this study. Implementation details of some subsystems such as transmitter and receiver are also given. In Chapter 6, the result obtained in the thesis has been discussed and some suggestions given for future work.

## **CHAPTER 2**

### **LASER SOURCES FOR RANGE FINDING**

Several types of laser sources are used in range finders. The choice of a particular laser source depends on the type of application (short range or long range measurement), required power output, pulse duration. Features and performances of various sources are briefly described below. Different types of laser sources used in range finders are reviewed in this chapter.

#### **2.1 SOLID-STATE LASERS**

All optically pumped solid state lasers consist essentially of a medium capable of producing optical gain, situated in a resonator which produces a positive optical feedback. The laser medium is usually fabricated in the form of a rod, and for real higher output energies, slabs and discs have been used. The dimensions of a typical laser rod used in a range finder lie between 3 and 7 mm diameter by 30 to 75 mm length. Considerable development effort has been expended upon the design of efficient techniques for optically pumping solid state lasers. The coupling of the output from the lamp into the laser rod is most efficiently achieved using an elliptical cylinder. The spectral emission from the pumping lamp must be optimized so as to match the absorption bands of the active ion. Having pumped the laser rod into a state in which it is capable of producing optical gain, positive feedback has then to be applied in order to create optical oscillations. This is most simply done by the use of two plane mirrors which are aligned to be perpendicular to the rod axis and accurately parallel to each other. However, a solid-state laser constructed with such a simple resonator generates a train of random output pulses. They arise because of rapid frequency jumps between various transverse and axial modes which the resonator can support within the amplification bandwidth of the material. Such a temporal output is almost useless for laser range finding applications. Hence some

techniques must be used to control the time evolution of the pulse stream. There are three techniques which are used for the control of the pulse development in range finding applications, viz., Q-switching, cavity dumping and mode locking. These techniques are briefly discussed below.

### **2.1.1 Q-SWITCHING**

With the simple resonator described above the optical gain in the medium increases with time up to the moment when the gain just balances the optical loss in the resonator. At this point the gain saturates and any further increase in population inversion is converted into optical output by stimulated emission. The dynamics of the balance between the population inversion and the radiation field inside the resonator is complex and leads to the random and complex pulse described above. If the feedback produced by the mirror is destroyed by the insertion into the resonator of an optical switch capable of switching the cavity Q-factor, laser oscillations can't then build up, and the gain goes on increasing with continuing pumping excitation. The gain will eventually reach an upper limit which will be determined by higher order process which compete for the population inversion. This could arise from depletion due to amplified spontaneous emission or from the onset of parasitic oscillations produced by unintended reflections (such as polished walls of the rod). The optical gain can thus be very much greater than that at which oscillation would occur in the absence of the switch. Suppose if the switch could be opened instantaneously, or at least in a time which is comparable to a few transits of the resonator. The photon flux would then start to build up from spontaneous emission noise very much rapidly than in the case of the uncontrolled resonator. Analysis of the dynamics of the process shows that, in principle, all the energy stored in the inverted population can be converted into radiation in a single optical pulse. The peak power and duration of Q-switched pulses are functions of initial gain and the dimensions of the resonator. Peak powers of the order of 1 to 10 MW in pulses lasting between 10 and 100 ns are easily obtained by this technique.

### **2.1.2 CAVITY DUMPING**

In this case, depending upon the gain of the laser medium and the characteristics of the resonator, the Q-switching technique can produce pulses with durations lying between 10 to 100 ns. The ranging accuracy which can be attained using such pulses is at best of the order of a few meters. For some applications a shorter pulse is desirable. A crude technique which has been used is simply to chop a short portion from a Q switched pulse by a second electro-optic switch outside the cavity. However, this is a very inefficient technique. A more satisfactory method is to use the cavity dumping approach. It is referred in literature as the pulse-transmission mode or PTM. This is essentially a variant on the Q-switching technique and uses slightly different layout for the resonator. As before, the inversion is allowed to build to its maximum value with the switch closed. When peak inversion is achieved, the switch is opened and the flux builds up inside the resonator. However, the reflectivity of the resonator mirrors are both high and so little radiation is allowed to be coupled to the outside world. The flux inside the resonator thus goes on building up until all the population inversion is converted to radiation via stimulated emission. At the instant of maximum flux, the switch opens a second channel which has very little loss, and thus all the radiation stored within the cavity is coupled out in a time comparable to a round trip between the mirrors. The switch obviously has to be able to make the transition between its various states in a time which is short compared with the resonator lifetime. Electro-optical switches are generally used in practice, and changes of the state of the polarization of the stored radiation are used to achieve the rapid output coupling. Using this technique, pulses down to 1 to 2 nanoseconds can be produced, which improves the range accuracy achievable to a few decimeters.

### **2.1.3 MODE LOCKING**

In order to achieve the ultimate precision in ranging accuracy, pulses produced by the mode locking technique must be employed. Here again, a switch inside the resonant cavity is used. But in this case the transmission of the switch is modulated with a period corresponding to the round trip time of photons within the cavity. There are two ways of considering the effect of this modulation on the light within the resonator. In the temporal case, the changing transmission of the switch tends to bunch the photons into packets which suffer minimum attenuation in their transit between the mirrors. In the frequency case, the action of the switch

is to produce a coupling between the different axial modes which the resonator supports within the amplification bandwidth of the laser material. The resultant effect is that the phases of these different frequency components correspond to the Fourier spectrum of a short pulse bouncing backwards and forwards between the mirrors. The width of the pulses thus has a minimum value which is set by the Fourier transform of the amplification bandwidth of the material. In practice the pulse width achievable depends upon the gain of the laser, the parameters of the cavity and the characteristics of the switch. Pulses with width in the region between a few tens of picoseconds and a few nanoseconds can be produced. For laser ranging applications, a single pulse would be removed from a mode-locked pulse train using an electro-optic switch and then the output energy increased to a usable level by a series of amplifiers.

#### **2.1.4 TYPES OF SOLID-STATE LASERS**

There are only a few materials that are capable of reasonably efficient operation at room temperature. The choice of active ion lies essentially between  $\text{Cr}^{3+}$ ,  $\text{Nd}^{3+}$ ,  $\text{Er}^{3+}$ , and  $\text{Ho}^{3+}$ . The first laser range finder was based on ruby which is single-crystal aluminium oxide doped with about 0.05%  $\text{Cr}^{3+}$ . This material is relatively inefficient and thus requires an input energy of several hundreds of joules. It is being replaced in most applications, particularly where the range finder is required to be portable, by materials doped with the  $\text{Nd}^{3+}$  ion. A large number of host materials for the ion have been investigated, including various glasses. The most popular is yttrium aluminium garnet,  $\text{Y}_3\text{Al}_5\text{O}_{12}$  (known as YAG), which is grown in single crystal form by a complicated process. YAG laser rods are therefore relatively expensive when compared to glass. The YAG as a laser material is attractive due to its high optical efficiency and excellent mechanical properties. By careful design of the pumping enclosure, it is possible produce high efficiency lasers. The mechanical properties of YAG which makes it an ideal laser material are its high mechanical strength and resistance to fracture, its excellent thermal conductivity and resistance to breakdown in high optical field. Depending on the input energy requirements either krypton or xenon discharge lamps. The main disadvantage of Nd:YAG as a source of laser power is that although the wavelength of radiation is beyond that of the human visible range, it can nevertheless be focussed on the retina and thereby cause damage.

## **2.2 GAS LASERS**

The only relevant type of gas laser is that in which the energy required to produce the population inversion of the gas is provided by an electrical discharge through the gas. Of the pulsed gas lasers only the CO<sub>2</sub> laser is attractive as a range finder source. For CW systems He-Ne and CO<sub>2</sub> lasers are used.

### **2.2.1 PULSED CO<sub>2</sub> LASER SOURCES**

Thermal imagers operate in the 8-14 $\mu$ m band which utilize the small variations of temperature and emissivity of objects near to the ambient temperature to produce images without the need for external sources of illumination. There has been a search for compatible laser source of radiation for range finding. The requirement is an equipment to measure the range of any target which can be distinguished by the imager and this would include for example an ability to penetrate mist and smoke. This coupled with the desire to operate range finders which are eye safe, has led to an interest to possible ways of using CO<sub>2</sub> lasers for range finding. The CO<sub>2</sub> molecule has an emission band which falls in the middle of the thermal window, and spans a range from 9.1 $\mu$ m to 11.28 $\mu$ m, with its strongest emission arising on the P(20) line at 10.59 $\mu$ m. It is also by far the most efficient of the gas lasers. For example, in the case of a low pressure CW laser the efficiency can be as high as 20%, but for pulsed lasers 5% is typical. High pulsed output powers require high pressures to increase the number of molecules contributing to the emission. However, this leads to the problem of achieving laser action with a pulsed discharge at high pressures.

The creation of uniform discharges in gases at pressures approaching one atmosphere is difficult because, once ionization occurs at some point the discharge tries to build up there to create an arc. Researchers showed that a uniform discharge could be created by transverse excitation between an array of resistively loaded metal pins and a flat bar. Lasers with such arrangements are called transversely excited, atmospheric-pressure (or TEA) laser. Generally the TEA laser is fed from a low-inductance capacitor charged to about 25kV. Initially the capacitor is isolated from the laser by a triggered spark gap. When the spark gap is fired, a subsidiary capacitor produces a discharge between the trigger wires and the cathode. This created UV radiation, which generates a uniform cloud of electrons in the gap between the

electrodes, thereby initiating the main capacitor to discharge. The population inversion produced by the discharge is generated so quickly that it has a similar effect to Q-switching in a solid-state laser and the radiation is produced in a pulse lasting about 60ns. For a discharge length of 250mm and an input energy of 2.5J, such a laser produces a peak output power of about 250kW [1].

The TEA laser provides a practical source for use in compact direct-detection systems which are required have ranges up to about 10km. This range may be increased to some extent by using lasers with even greater output power but the range increase is a rapidly diminishing function of power because of the  $\exp(-2kR)$  factor in the signal strength produced by the atmospheric attenuation coefficient  $k$  and the change over from  $1/R^2$  to  $1/R^4$  dependence of signal strength on range  $R$  as the target ceases to fill the beam. Thus further range increments are possible only by utilizing the greater sensitivity offered by the use of heterodyne detection. This in turn places demand upon the characteristics required of the transmitter source. Ideally it should produce a high-power at a single, stable frequency, which is offset by a fixed value (the IF) from a stable CW source which acts as a local oscillator (LO). The axial mode of laser separation for a laser resonator length  $L$  meters is  $c/2L$  Hz, where  $c$  is velocity of light. The pressure broadened bandwidth of a TEA laser, when operated at atmospheric pressure, is about 3 GHz, and so a resonator 300 mm long could support six axial modes within the amplification bandwidth. One possibility is to use a short resonator capable of oscillating in only one mode.

### **2.2.2 CW GAS LASERS**

Popular CW gas lasers used in range finders are He-Ne and CO<sub>2</sub> lasers. The He-Ne red laser emits at 632.8 nm. This laser is available in various power ranges varying from 1 to 25mW and is applied in surveying range finders. Portability is the main concern and hence the low power versions are most widely used. These laser sources are about 250mm long and 50mm diameter and they require dc drive voltages of hundreds or thousands of volts. These lasers are extensively used for a variety of applications, and hence reliable, long-life, sealed-off versions are available commercially.



CW versions of CO<sub>2</sub> lasers are available in various powers ranging from fractions of a watt to up to many watts (even kilowatts), with lengths ranging from a fraction of a meter upwards. Single longitudinal mode outputs are available from the shorter lasers and this makes them suitable as frequency-stable sources for heterodyne detection systems.

## **2.3 SEMICONDUCTOR LASERS**

The most commonly used semiconductor laser in rangefinders is the GaAs laser. Semiconductor lasers are attractive because they are small and are efficient sources capable of being rapidly modulated by varying the drive current. The radiation wavelength are in the range of 0.8 to 0.9 $\mu$ m. The average power output is generally a few milliwatts to a few watts and the pulse length of the order of 10 to 15nsec. Laser action is obtained by population inversion in the vicinity of a p-n junction, forward biased to produce carrier injection. These sources have efficient room temperature operation. Also, they have high efficiency and high repetition rate and hence suitable for most civilian as well as military applications.

## CHAPTER 3

### REVIEW OF LASER RANGE FINDERS

This chapter reviews Laser range finders (long and short ranges). Different types and techniques employed in these range finders are reviewed after a brief discussion on the basic principle of long range measurement.

#### 3.1 BASIC PRINCIPLE OF LONG RANGE MEASUREMENT

Time of flight (TOF) measurement is the simplest and easiest way of measuring long range. The range R in meters is calculated from

$$R=(CT_R)/2 \quad (3.1)$$

where C is the velocity of light ( $= 3 \times 10^8$  m/s),  $T_R$  is the time elapsed between the departure of the light pulse from the transmitter and its arrival at the receiver.

The principal elements of a pulsed laser range finder are shown in Fig.3.1 and a general block diagram of the same in Fig.3.2 [1]. Majority of these Range Finders use an optically pumped solid-state laser as the source of transmitter power (pulsed CO<sub>2</sub> lasers systems are also used). In general, the principal optical elements of a typical ranging system as shown in Fig.3.1) are

- 1.Sighting Telescope
- 2.Transmitter
- 3.Receiver

Overall system performance depends on these three subsystems and how they are realized physically. The sequence of events in a typical pulsed laser range finder is as follows. The sighting Telescopes is carefully aligned to point at the target and then the transmitter pulse is initiated. A small fraction of the energy from the pulse is picked up from the laser diode and is fed to the fast photodiode in the receiver circuit. The output from the

# TRANSMITTER

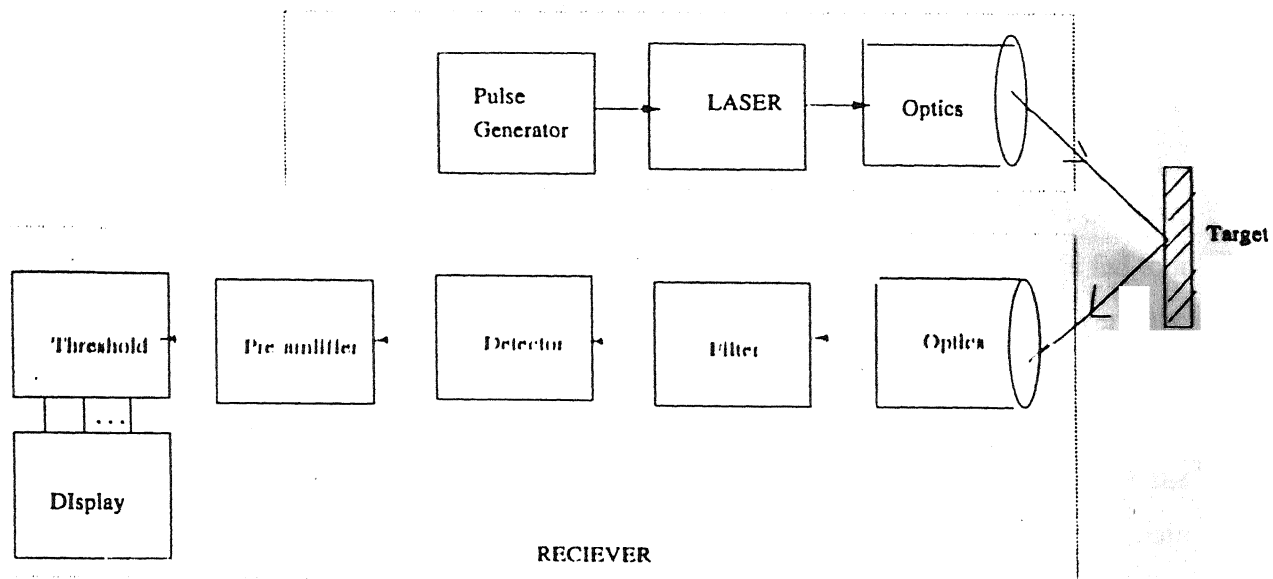


Fig.3.1 Principal elements of a pulsed laser range finder

# TRANSMITTER

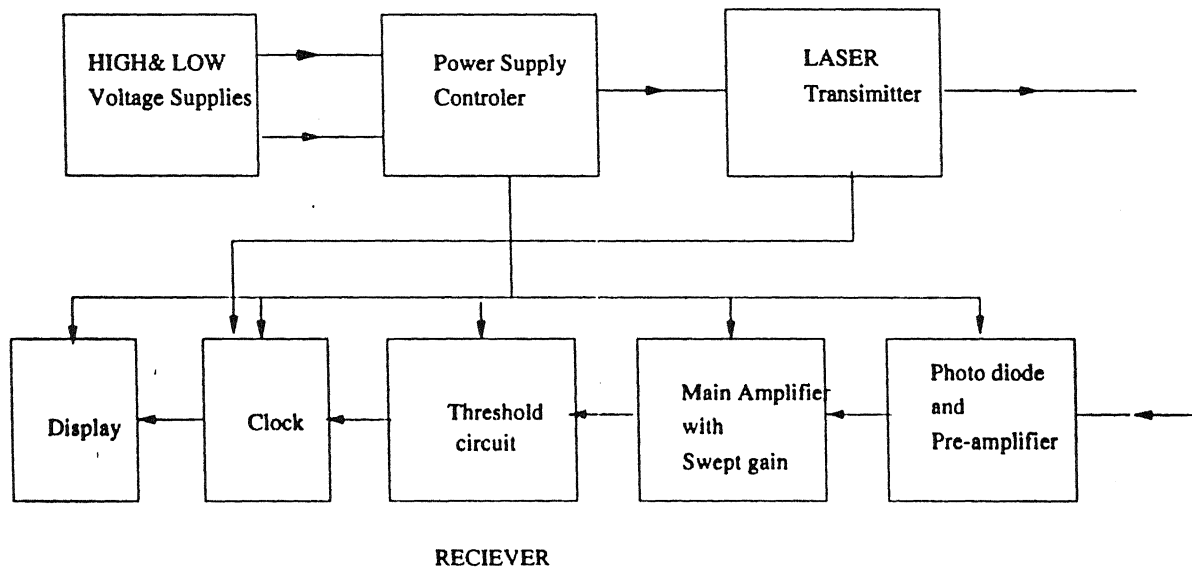


Fig.3.2 General block diagram of a pulsed laser range finder

photodiode initiates a high speed counter which is clocked by pulses from a quartz – controlled oscillator. A small fraction of the energy reflected from the target is collected by the receiver lens, which is focussed on to the detector. In order to reduce the energy reaching the detector from unwanted broadband sources within the receiver field of view, a suitable narrow band interference filter is used. The output from the detector is fed to a preamplifier. The preamplifier is generally of transimpedance design, which converts the current developed by the detector in high impedance to a low impedance output which minimizes the additional noise introduced by the conversion process. Signal level is further increased by a main amplifier. In order to compress the dynamic range of the signals produced at the output it is normal practice to sweep the gain of the main amplifier as a function of time so that strong signals from near by targets are amplified less than weaker signals from more distant ones.

The amplified signal is then applied to a threshold comparator. If the signal exceeds an internally set voltage the clock is stopped. The threshold has to be set carefully, so that noise signals alone only very rarely cross the threshold to create false alarms, and yet must not be set so high that there is an appreciable probability that true signals will be missed. For a satisfactory statistical performance, the amplitude signals-to-noise ratio (SNR) need to be set much larger than unity. If the clock frequency is chosen correctly the number of clock periods stored in the counter can be simply related to the range of the target. For example if the clock frequency is set at say, 30MHz, light will travel 10m in one clock cycle and the range resolution of the instrument will be  $\pm 5\text{m}$ . In some designs the system can cope with more than one pulse exceeding the threshold value, in which case the clock is not actually stopped by the signal crossing the threshold level, but instead the clock count at each occurrence is stored and are read out in sequence at the end of the ranging operation. It is then left to the judgement of the operator to decide which is the true range to the target. Laser ranging systems use direct detection in most of the cases and <sup>in</sup> some cases they employ heterodyne detection, especially when CO<sub>2</sub> laser is used as the transmitter source. The common laser sources used are GaAs laser diodes, Nd:YAG lasers and CO<sub>2</sub> lasers. Different ranging systems making use of the above three lasers are reviewed below.

## **3.2 RANGE MEASUREMENT SYSTEM USING Ga As LASER**

### **DIODES**

Ga As injection Lasers radiating in the wavelength region of  $8400\text{-}9000\text{\AA}$  are at times used in pulsed ranging systems. There are several attractive features of Ga As which are useful in several applications, such as ranging, altimetry and space rendezvous systems, requiring limited range and high pulse repetition rates. The major features of GaAs laser systems are [2-4]

1. small size and weight
2. Direct current modulation enabling conversion to infrared radiation with high internal efficiency
3. efficient room temperature operation
4. ability to modulate with short pulses and high frequency waveforms
5. simple and rugged in construction
6. high pulse repetition rate capability

In comparison to solid state their output is relatively low, typically of the order of 10 to 100W. The radiation wavelength of GaAs is temperature dependent (it shifts at  $0.25\text{nm}/^\circ\text{K}$  at room temperature). So depending upon the application some temperature stabilization techniques are used. The spectral width is between 1 to 2nm caused mainly by multimode operation and temperature increase while the current pulse is being applied. The multimode occurs because the diode current pulses are 2 to 4 times larger than the threshold current for laser action. The light emitted from the laser diode is diffraction limited for the smaller dimension of the *p-n* junction (typical junction thickness is  $3\mu\text{m}$ ). The angular beam spread of about 2nm for the larger dimension (junction width) is given by the different modes in the Fabry-Perrot type of the *p-n* junction. Small beam divergence can be obtained by using collimating lens. To handle the high currents necessary for laser action in room temperature laser diodes, different approaches for the pulse generators are possible. Commonly used switching element in the pulse generator include SCRs, Transistors in avalanche mode, Cold cathode tubes,

mercury-wetted relays and specially built mechanical contacts. The block schematic of a typical GaAs laser range finder is shown in Fig.3.3.

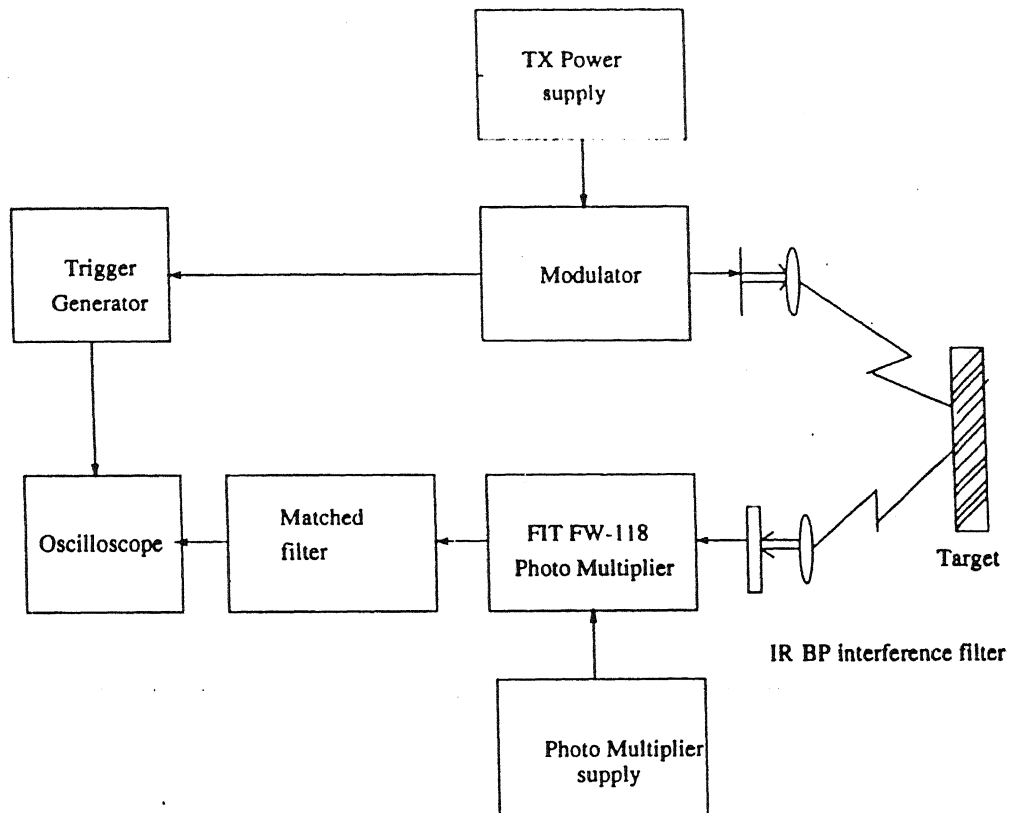


**Fig.3.3 Block diagram of a GaAs laser range finder**

In the receiver section the photo multiplier tubes (PMT) are generally used as the detector whose dark current at room temperature is of the order of 1pA and internal current gain of of 50,000 [2,3]. The interference type IR band pass filter is incorporated in the detector assembly to reduce the background radiation. A video amplifier is used to amplify the output of the PMT, with typical gains of the order of 50dB, and bandwidths

of about 40MHz. Silicon avalanche photodiodes are also employed in some applications. One such application is given in Ref.[4].

**PERFORMANCE:** The range capability of GaAs laser radar depends upon system parameters and operation environment. Injection Laser diodes capable of coherent radiation in the visible region would considerably improve the response. Silicon and Germanium avalanche photodetectors with more sensitivity in the near infrared are preferred choices. There are two ways to improve the range performance, one is by increasing the transmitter signal power and the other by increasing the sensitivity of detector. Injection lasers have lower powers as compared to other lasers. With the available power output a further increase of the maximum range is only possible by increasing the sensitivity of the detection system. This may be achieved by signal processing techniques without increasing the time necessary for measurement. In general, the limited power output restricting the maximum range capability, represents the most serious handicap of Injection laser radars.

### **3.3 RANGE MEASUREMENT SYSTEMS USING CO<sub>2</sub> LASERS**

Range measurement systems using CO<sub>2</sub> lasers are generally based on TOF method. Making use of high power lasers operating at a wavelength of 10.6 $\mu$ m and peak powers of the order of several kW. Other CO<sub>2</sub> lasers ranging systems employ FM-CW radar techniques. The main advantage of CO<sub>2</sub> lasers is that even though they emit high powers eye safety is generally maintained for commonly used transmitter aperture diameters. Also, the pulses emitted by this can easily transmit through mists and hazes. Some of the CO<sub>2</sub> laser ranging systems are briefly reviewed below.

A pulsed CO<sub>2</sub> laser ranging system has been reported by Taylor *et al* [44]. They named this system as Ferranti 303 which uses a Marconi Avionics tube with a peak power of about 300kW and pulse width of 60ns (full-width at half maximum). The transmitter beam with had a full-cone divergence less than 0.7 mrad. The receiver aperture had a diameter of 150mm and the detector was a lead-tin telluride photodiode operated at 80K by a Joule-Thomson compressed-air cooling system. Range performance of 5km with an accuracy of  $\pm 5$ m was achieved for natural targets.

Another pulsed CO<sub>2</sub> laser ranging system reported made use of a CO<sub>2</sub> TEA laser with 400ns pulse width and 30kW peak power [42]. Ranges of 2km were achieved with this system.

Yet another range measurement method using CO<sub>2</sub> lasers makes use of the FM-CW Radar technique [43]. In conventional FM-CW radar theory, the range to a stationary target is determined by the frequency difference between the signal returned from the target and the frequency then present at the transmitter. If the echo signal is homodyned with a portion of the transmitter signal in a nonlinear detector, a beat note  $f_b$  will be produced, which is proportional to the target range  $R$ . If the transit time of the energy travelling to the target and back is smaller than the time involving the maximum unambiguous range  $R_{max}$  ( $=c/8f_m$ , where  $f_m$  is the modulating frequency), this beat frequency is related to the target range by

$$f_b = 4Rf_m\Delta f/c \quad (3.2)$$

where  $\Delta f$  is the full width of the frequency excursion. In this application they used a 3W, CW output and a piezoelectric transducer was used to produce a  $\Delta f$  of 20MHz at 45Hz modulation frequency. Sinusoidal beat frequencies of 1500 and 2780 Hz were measured corresponding to ranges of 62 and 115m, respectively.

The schematic diagram of a CO<sub>2</sub> laser range finder making use of heterodyne detection and chirp pulse compression is shown in Fig 3.4 [5]. In this range finder an acousto-optic modulator (using a surface acoustic wave device) is used in the transmitter to superimpose a precise, electronically generated modulation on the CW laser. The modulating waveform consisted of a train of constant amplitude pulses of 4 $\mu$ s duration with linear frequency modulation from 53 to 67 MHz repeated every 33 $\mu$ s. Such individual pulses are termed as 'chirp pulses'. The return beam from the target is mixed on the detector with a portion of the frequency-swept transmitter beam acting as a local oscillator.. The frequency of the signal at detector output is then related to the target range. Separate transmit and receive apertures of 50mm diameter were used. The fractional accuracy of range determination by this scheme was typically limited to about



10% by the inability to produce precisely the required linear variation of frequency with time. Signal-to-noise ratio in this system was augmented by adding successive returns in a digital integrator. A maximum range of 10km was obtained. Because of the chirp signal processing there existed a range error for moving targets of typically 8m/sec radial velocity.

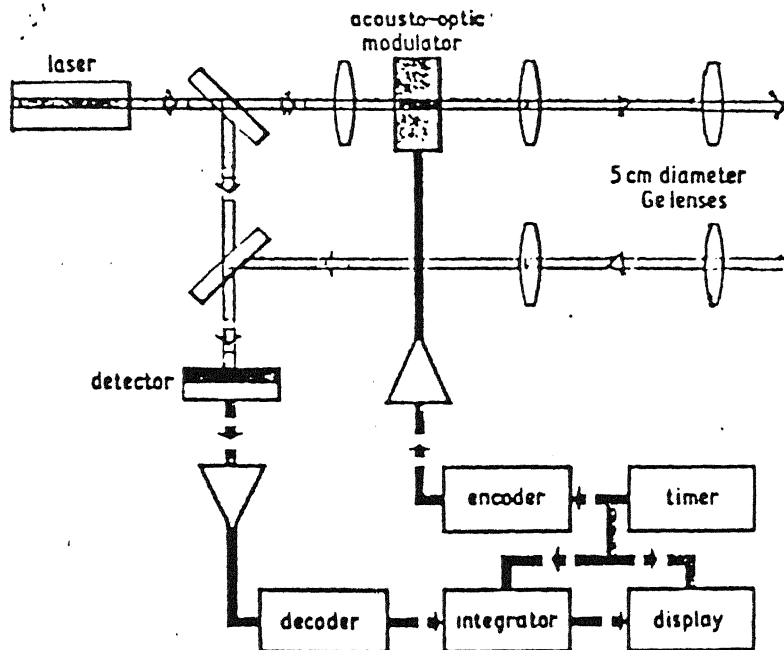


Fig.3.4 Schematic diagram of a CO<sub>2</sub> laser range finder making use of heterodyne detection and chirp pulse compression

Heterodyne detection enjoys a real advantage over direct detection when the receiver aperture size must be minimized. For example, to counter-balance a typical factor of 80 in detector sensitivity, the direct detection receiver would need about 9 times the aperture diameter. Another advantage of a heterodyne-detection system is the ability to determine target velocity from any Doppler frequency shift.

### **3.4 RANGE MEASUREMENT SYSTEM USING Nd:YAG LASERS**

Nd :YAG (Neobidium Yttrium Alluminium Garnet) lasers form a class of solid-state lasers which are very popular in several applications. Their emission wavelength is 1.06  $\mu\text{m}$ . These lasers are becoming popular choices in laser ranging systems due to their compactness and other desirable features for long range measurements. The success of YAG as a laser material arises from its combination of optical efficiency and excellent mechanical properties. By careful design of the pumping enclosure, it is possible to produce an efficiency, measured in terms of the optical energy produced compared with the energy in the capacitor, in the excess of 2% as compared to 0.05% of ruby. The only major disadvantage of the Nd:YAG as a source of laser power is that even though wavelength of radiation is beyond the human visible range it can cause damage to the eye if focussed on to the retina [1].

A hand-held Nd:YAG laser based range finder has been reported for use in military applications [1]. This range finder emits optical pulse energy of 4mJ in a 1.5mrad beam. Sighting of the target is achieved by a x7 telescope. The telescope also focuses the returned laser energy on to a silicon APD via a dichroic beam splitter. The equipment has a ranging capability of about 9km under conditions of good visibility, with a range resolution of  $\pm 5\text{m}$ . A 4-digit LED display presents the range to the operator. Similar equipment is available for battle tank applications. One such system, called LF-11, uses a Nd:YAG laser with a peak power of 2MW and pulse width of 5ns for range measurements from 500m to 10km[1].

Another laser ranging system used for defence applications is the Ferranti airborne Nd:YAG laser rangefinder. This equipment is part of the weapon aiming systems of Jaguar, Harrier and Tornado aircrafts of the RAF, UK [1]. Here an electro-optically Q-switched Nd:YAG laser capable of operating at 10 or 20 Hz is used.

Other laser ranging systems are also reported. One such system used pulse-Doppler laser radar making use of laser diode pumped Nd:YAG oscillator of extreme frequency stability. The output of the oscillator was passed through a permanent-magnet

optical isolator and then gated and frequency shifted by an acousto-optic modulator before amplification. The linear amplifier generated high-peak-power pulses, which were then transmitted through a parabolic mirror. Signal returning from distant targets to the mirror is collected in a single-mode optical fiber, mixed with the oscillator output and detected [7]. Signals from clouds at a range of 2.7km and from atmospheric aerosols at a range of 600m were detected.

Yet another recent system used Nd:YAG with a pair of streak cameras to achieve accuracy several millimeters in long range measurements [6]. In this the basic radar system consisted of a Nd:YAG laser , a KDP doubling crystal, a KD\*P tripling crystal, a frequency-stabilized master oscillator, an optical-clock generator, two matched streak cameras, and an output-input telescope system. The laser is Q switched and mode locked and outputs a burst of pulses at 500Hz repetition rate. Each pulse in the burst has a pulse width of less than 100ps (FWHM). A single pulse is extracted from each burst by use of a Pockels cell. The train of single pulses, which has a fundamental frequency of  $1.064\mu\text{m}$ , is then directed through KDP second-harmonic generating and KD\*P third-harmonic generating crystals producing 532 and 355nm wavelength pulses, respectively. All three wavelength pulses emerge simultaneously. The three-wavelength ranging pulses are combined and then directed into the beam expander and launched through the sending telescope toward the target. This system achieved a resolution better than 1cm over a range of 30km.

Another Nd:YAG laser ranging system reported is called PATS (the Sylvania Precision Aircraft Tracking System) which is used for tracking and position determination of cooperative targets such as aircrafts [45]. This system is capable of measuring azimuth, elevation and range of a target at sample rates up to one hundred measurement sets per second. It used a Q-switched, flash-pumped Nd:YAG laser having a pulse width of 25ns, developing 1MW peak power in a 10mrad beam at a rate of 100pps. The beam, which is coaxial with the receiver, is directed to the target by an azimuth-elevation mirror mount. The return beam is imaged on separate ranging and

tracking receivers. The ranging receiver is capable of measurements with range accuracies of  $\pm 15\text{cm}$ .

### **3.5 SHORT RANGE MEASUREMENT SYSTEMS**

In the case of short-range measurements many techniques are used to measure the range. Some of them are

1. Interferometric technique
2. Phase-shift measurement technique
3. Optical triangulation method

#### **3.5.1 INTERFEROMETRIC TECHNIQUE**

This method is used to measure small distances with high accuracy. The basic principle involved is to split a beam of monochromatic coherent light from a laser into two parts, and to bounce the beams around a bit and then recombine them with a screen, optical viewer, or sensor array. The beams will constructively, or destructively interfere with each other on a point-by-point basis depending on the net path length difference between. This will result in a pattern of light and dark fringes. If one of the beams is reflected from a mirror or corner reflector whose position is to be measured precisely, then counting the passage of fringes can provide fairly accurate measurements. We review some methods with use some special techniques which are different from the commonly used interferometric techniques.

One such system used a method for measuring distance larger than the wavelength of light with an interferometer using a laser diode [8]. This method uses the fact that the wavelength of the emitted light of a laser diode varies in proportion to the diode's injection current. The phase difference between the two interfering beams varies due to the sinusoidal variation of wavelength. The variation of the phase difference is detected by optical heterodyne method. The magnitude of the variation is proportional to the measuring distance and the light wavelength shift. If the wavelength shift is known, a

distance larger than the wavelength can be obtained from measurement of the phase variation. This method may be thought of as a kind of multiwavelength interferometry using a single light source. Using this method they were able to measure ranges of the order of a few mm with an accuracy of a few microns.

Another variation of the above technique was reported where a frequency modulated diode laser was used to measure ranges of the order of a few centimeters with a resolution of a few microns [46]. In Ref.[8] it is shown that sinusoidal detuning of the laser wavelength yields an interference signal proportional to

$$A \cos(2\pi\Delta\nu t + 2\pi L\Delta\lambda/\lambda^2) \quad (3.3)$$

In the present system  $\Delta\nu$  is a difference frequency of 455kHz generated with two acousto-optic modulators. The periodic wavelength variation is denoted by  $\Delta\lambda$ , and  $\lambda$  is the average wavelength.  $L$  is the optical path difference (OPD) in the interferometer that is to be measured. A phase comparator is used to measure the time-varying phase  $2\pi L\Delta\lambda/\lambda^2$ . This phase term is filtered with a bandpass filter whose center frequency is set to the modulation frequency of the wavelength modulation. The amplitude of the filtered periodic phase variation is measured, which is proportional to the OPD. Once  $\Delta\lambda$  and  $\lambda$  are known, the absolute value of OPD can be determined.

### **3.5.2 PHASESHIFT MEASUREMENT TECHNIQUE**

Range measurement can also be done by measuring phase shift between the transmitted and the received signals. One paper gave a technique using a frequency-modulated optical source. In this technique the light reflected by the target is coherently detected to obtain the frequency dependence of the round-trip optical phase shift. Laser diode was used both as a frequency tunable source and an optical-phase discriminator [9].

The distance from the laser to the reflective target  $L$  can be determined from the laser frequency deviation  $\Delta f$ , which produces one full cycle of phase change in the light fed back into the laser from the target. The two quantities are related by the equation,  $\Delta f = c/2L$ , where  $c$  is the speed of light. The laser frequency is tuned by modulating the

laser-diode drive current. It is known that an increase in drive current shifts the laser emission to a slightly longer wavelength by increasing the laser cavity's temperature and refractive index. The dependence of the reflected light's phase on the source frequency is obtained by monitoring the laser diode output power while tuning the laser frequency. The external reflector effectively modulates the reflectance of the laser diode's front facet. The reflective target and laser front facet form an external cavity of length  $L$ , where  $L$  is much larger than the optical length of the laser diode cavity. When subject to feedback from the target, the laser diode will lock to the external-cavity resonant frequency closest to the frequency at which the laser would operate without feedback. When the laser's free-running frequency is tuned by modulating the diode drive current, mode hops occur at intervals of free-running frequency equal to the frequency difference between consecutive external cavity modes,  $c/2L$ . Range is determined by counting the number of mode hops  $N$  that result from a laser frequency deviation of magnitude  $\Delta F$ . The distance to the target is given by  $L=Nc/2\Delta F$ . The resolution in range is  $\Delta L=c/2\Delta F$ . For a laser frequency excursion of 50GHz,  $\Delta L=3\text{mm}$ . This method has been used to measure distances up to 1.5m.

### **3.5.3 OPTICAL TRIANGULATION METHOD**

This method is commonly used to measure the smaller distances in laboratories and even in 35mm cameras. It is based on trigonometric principles and the measured distance is obtained by using the difference in angles of the line of sight from a source (LED/LASER) to the scene and back to a detector mounted a few centimeters away. As the distance is reduced, the angle increases. This is coupled to the lens focusing mechanism in a camera. The use of a well collimated laser would increase both the maximum useful distance and resolution of the system [10]. These techniques are used mainly for robotic applications.

The dynamic implementation in the form of a laser scanner can actually be used to implement a 3-D profile measurement system. If a laser beam is scanned across a 3-D object, and the spot is viewed (by optical sensors) from two different locations, it is possible to determine the instantaneous distance to the spot (on the object). This can be

reduced down digitally (using a pair of slow CCD cameras) or in analog domain using 4-quadrant photo diodes. This method is generally used in factory automation, control systems and visible sensor in robots [22].

In the case of short range measurement, time-of-flight (TOF) method is also used. High resolution of the order one centimeter can be achieved by this method. The light reflected by the target is coherently detected to obtain the frequency dependence of the round trip optical phase shift. Considerable device simplification is achieved by using a laser diode as both the frequency tunable source and an optical phase discriminator

## CHAPTER 4

### SYSTEM CONSIDERATIONS OF LASER RANGE FINDERS

While designing laser range finders one needs to consider many factors based on the type of range measurement (long range/short range). The main system considerations are based on the selection of sources (transmitters), type of detectors (receivers), signal processing equipment, and proper lens systems. The main transmitter source for any meaningful range measurement is the laser source. The choice of a suitable laser source depends on available peak signal power output, type of waveform to be generated; (pulsed/CW), and the length of the pulse. The choice of transmitter also depends on whether the radar operates from fixed land sites, mobile land vehicles, ships, aircraft or spacecraft. Other considerations include the size, weight, high-voltage, X-ray protection, modulation requirements, etc. Transmitter is a major part of a laser ranging system; hence its size, cost, reliability, maintainability are to be considered.

The function of radar receiver is to detect the desired echo signals in the presence of noise, interference, or clutter. It must separate wanted signals from unwanted, and amplify the signal to the level where the target information can be extracted. The design of receiver depends not only on the type of echo to be detected, but also on the nature of noise, interference, and clutter echo's with desired echo to compete. Maximum range requirements demands maximizing the signal to noise ratio at the output. Protection must be provided against overload or saturation, and burn out from nearby interfering transmitters. Timing and reference signals are needed to properly extract the target information. The choice of detectors based on response time, sensitivity, The upper limit of the response time is determined by the range accuracy, and modulation band width of the received laser signal.



In this chapter we will consider various aspects of laser ranging systems including laser transmitters, detectors, atmospheric transmission, electronic circuitry, optics, etc.

## **4.1 ATMOSPHERIC PROPAGATION**

When we transmit the light pulse to a particular direction the reflected echo signal is not the same as the transmitted one as it reaches the receiver, because it underwent many changes. The propagation of the signal is affected by change in refraction caused by an inhomogeneous atmosphere and attenuation by the gases constituting the atmosphere. It is also affected by other external noise sources, viz. solar, cosmic, u.v radiation, etc. Some of these factors affecting the signal propagation is discussed here.

### **4.1.1 ATTENUATION: [2]**

The transmission factor for the two way path to and from a target at distance R is given by  $R = \exp(-2kR)$ , where k is the total absorption coefficient which is the sum of absorption and scattering contributions  $k_a$  and  $k_s$ ;  $k = k_a + k_s$ .

## **MOLECULAR ABSORPTION**

The spectral range of interest for laser range finding is limited by atmospheric absorption, at one end by ozone absorption below 300nm and at the other end by water vapour beyond 14 $\mu$ m. In between, the attenuation coefficient has an extremely complex variation with wavelength. There are windows available in the visible and near infrared, in the 3-5 and 8-14 $\mu$ m bands. The contribution from molecular (Rayleigh) scattering is only about 0.01 km<sup>-1</sup> for the Nd second harmonics and becomes negligible at longer wavelengths.

## **SCATTERING AND ABSORPTION BY AEROSOLS**

Aerosols contributions can arise from solid particles (dusts, smokes etc) and droplets (hazes, mists, rain, fog, snow, hail, etc). Water droplets may nucleate on solid particles as humidity rises so that the distinction between solid and liquid aerosols is not always completely clear cut. It is difficult to predict the fact that the atmospheric aerosol is rarely uniform over the relevant distances.

## TURBULENCE

The optical perfection and uniformity of the atmosphere are destroyed by the turbulent and convective motion of air masses with different temperatures which result in a non-uniform refractive index. The index variations are due to atmospheric temperature inhomogeneities. The spectral density distribution of spatial variations occur with the change in the refractive index. There are several significant effects created by atmospheric turbulence. They are beam steering, breakup of a beam intensity fluctuations, transfers phase fluctuations. Transverse phase variations at the receiver caused by turbulence on the return path can be significant in a heterodyne-system in setting a limit to useful receiver aperture size.

Intensity fluctuations at the receiver plane arise because, as the turbulence evolves and alters the refractive index structure along the path, the blob pattern alters. These temporal variations have bandwidth of order  $v/(2\pi\lambda R)^{1/2}$ , where  $v$  transverse wind speed; with  $v=10\text{m/s}$ ,  $\lambda = 1.06\times 10^{-6}\text{m}$ (Nd laser) and  $R=5\times 10^3\text{m}$ , which comes out to about 55Hz

## 4.2 TARGETS

Here we consider two types of targets; a)co-operate targets, such as retro reflectors, and b)Non co-operative targets, such as trees, buildings, vehicles. etc. Here we'll consider the performance of the target on the basis of the returns at receiver input. The small divergence of a typical laser range finder beams means that targets often fill the beam. It is then useful to describe the magnitude of back-scattered return from a plane surface in terms of an effective lambertian diffuse reflectivity  $\epsilon$ , which is the return strength relative to that from a target which scatters 100% of the incident radiation with an angular distribution obeying Lambert's law. The quantity  $\epsilon$  varies with angle of incidence with respect to a particular surface. The back-scattered radiant intensity is provided by a surface with lambertian diffuse reflectivity  $\epsilon(\theta)$ , when illuminated at an angle  $\theta$  to its normal by a radiant flux of  $\phi$  watts, is then  $I=(\phi\epsilon\cos\theta)/\pi$  watts per steradian. Thus, if a plane surface at range  $R$  is illuminated normally by a laser of power  $\phi$ , the average power collected by a receiver of area  $A_r$  is given by  $P_r =[\phi\epsilon A_r/\pi R^2 \exp(-2kR)]$ , where the last term takes account of atmospheric extinction. For all this power to reach the detector, the field of view of the receiver has to be large enough to cover the illuminated area (i.e. has to be at least as large as the transmitter field of view). If the diffusely

reflecting target of area  $A$  does not fill the beam, the above expression must be multiplied by a factor  $(4A)/(\pi R^2 \theta^2)$ , where it has been assumed that the transmitter power is uniformly distributed over a cone with full cone angle  $\theta$ .

The diffused reflectivities of rough targets depends on the constitution and wavelength and to a lesser extent on the angle of incidence. They can vary widely on smooth surfaces which shows a marked variation with angle of incidence, being high near the specular condition and low away from it. The returns from non planar targets can in principle be obtained by integrating the effects of the inclined constituents. Measured returns are, however, often expressed in terms of an  $\epsilon$  that would apply if on the target illuminated were normal to the incident beam [3].

Retro-reflective targets are usually formed from corner cubes, i.e. three mutually perpendicular reflecting surfaces that have the property of returning incident rays back parallel to their incident direction. A small perfect retro-reflector presenting a circular area  $A'$  to the incident radiation returns a perfectly flat incident wavefront distributed over a diffraction – limited solid angle of order  $4\lambda^2/A'$ .

There is a vast difference between non-cooperative and cooperative (retro-reflective) targets. For example if a retro-reflective area of  $10^{-2} \text{ m}^2$ , behaves perfectly, it would return incident radiation of 1- $\mu\text{m}$  wavelength. over a solid angle of  $\sim 4 \times 10^{-10}$  steradian, whereas a 100% Lambertian reflector at normal incidence would give a backscattered intensity corresponding to distributing the radiation uniformly over  $\pi$  steradian. An equal area of the retro-reflector thus gives  $10^{10}$  more return signal. Array of retro-reflectors are often used to give omni-directional effectiveness and/or to increase the strength of the reflection.

#### **4.2.1 SPECKLE EFFECTS (SIGNAL FLUCTUATIONS)**

A consequence of the monochromatic nature of the laser emission is that, there are usually effects due to interference between the radiation scattered by different parts of the target. A diffusely scattering target is often modelled as an array of random phase scatters, and intensity at the receiver plane is non-uniform, forming a random pattern, called speckle blobs.

Speckle phenomenon is that, at the receiver plane, the amplitude at any point is a sample from a random process, namely, the sum of the large number of contributions from the scatterers, each contribution having a random phase and amplitude. The probability distribution of the amplitude is Gaussian. As the point of observation in the receiver plane is altered, the major effect is that the phase of the individual contributions alter; the resultant sum therefore changes. The displacement needed to change the intensity and phase significantly is the scale size  $\Delta$  of the speckle-blob pattern, and is given by  $\Delta \sim \lambda R/D$ , where  $D$  is the diameter of the illuminated area, assumed to be circular.

If the target surface moves, so as to either change the area illuminated or to change the relative phase of returns from different parts, the speckle pattern will also change. The time taken for the pattern to change significantly is the coherence time of the return, and significant in waveform design because long transmitted waveforms compared with the coherence time will be corrupted and ideal processing of detector output will be impossible (heterodyne detection cases only). If the target has a finite depth and the laser transmitter has sufficiently broad bandwidth, speckle fluctuations will be averaged. This often occurs for solid state lasers with typical natural targets.

## **4.3 RECEIVERS**

The function of radar receiver is to detect desired echo signals in the presence of noise, interference or clutter. It must separate wanted from unwanted signals, and amplify the wanted signals to a level where target information can be extracted. The design of a radar receiver not only depends on the type of waveform to be detected but also on the nature of the noise, interference, and clutter echoes in which the desired signal must compete. Here in optical range finders we have to consider so many factors while designing a radar receiver. The performance of the receiver also depends on the proper choice of optical lens system, type of detectors and further amplification stages.

### **4.3.1 OPTICAL DESIGN**

In the case of laser range finders the design of lens system plays an important role. Usually lens or mirror system will concentrate the incident radiation on to a photodetector. The receiver field of view and entrance aperture size will be an important design feature. For a

direct detection system, the field of view of the receiver is set by the detector size  $d$  and the focal length ' $f$ ' of the optical system, which leads to an angular field of view  $\theta = d/f$ . For a heterodyne system, the field of view is limited by a need for the aperture to gather in-phase contributions from all parts and mix them with the local oscillator, which leads to an angular field of view  $\theta \sim \lambda/D$ , where  $D$  is the aperture diameter.

### **4.3.2 PHOTODETECTORS**

The choice of photo detector depends mainly on the two factors, viz. the response time and the sensitivity of the receiver system. The upper limit of the permissible response time is determined by the accuracy required and/or the modulation bandwidth of the receiver signal. The response times in the range 1-100 nano seconds are generally required. Two types of detectors have been generally used. Photo cathodes (photo sensitive element in a photo multiplier), where the photo electrons are ejected into vacuum, and the photodiodes or photo conductors, where photo electrons are generated internally in a semiconductor. We need high value of quantum efficiency, defined as the number of photoelectrons produced for incident quantum of radiation. The response time of photo cathodes falls off rather sharply as the wavelength increases so that the sensitivity falls at the red end of the spectrum. In the case of semiconductor detectors, the excitation of the photoelectrons from impurities in the semiconductor (Si, Ge). The more useful semiconductor internal photo excitation mode now appears to be excitation of carriers from valance band to conduction band. This implies that the spectral sensitivity of the device is set by the band gap of the semiconductor. Hence generally detection material is chosen in such a way that to have small energy band gap.

The photo multipliers (where the photo cathode is conveniently combined with low noise, high gain amplification ) are generally used in ruby, Nd:YAG, CO<sub>2</sub> laser range finders. Silicon photodiodes or avalanche photodiodes (where the internal gain is provided by the electron-hole avalanche multiplication in the high field of the reverse biased PN junction) are generally used in GaAs laser range finders.

### **4.3.3 NOISE SOURCES**

The main sources of noise present in the receivers are the internally generated (dark current noise ) and the externally generated (background radiation ) ones. The principal random noise present in the output current of a photoemissive diode are the shot noise of the dark current and the photon noise due to incoming radiation signals. Both the noises are observed in the output current of the photo emissive surface and are indistinguishable if the photon arrival is random. Shot noise is due to fluctuations in the temperature-limited thermionic emission process and its magnitude is determined by the cathode material, area, and temperature. Photon noise is defined as the noise in the output current due to fluctuations in the rate by which radiation quanta acts on the photo cathode. It is the net effect of the fluctuations in both the incident power and emitted electrons [24]. When the quantum efficiency is less than unity, the random fluctuation in incident background radiation are negligible compared to those of the photoelectric emission process.

**Dark current:** The dark current is due to thermionic emission of the photo cathode. The total current is a function of the cathode area, work function and cathode temperature. If the cathode is cooled at 0°K and there is no background radiation, the detectivity of detector will be restricted only by the quantum efficiency, no matter whether the detection is coherent or non-coherent.

**Background radiation:** Any non laser radiation reaching the detector by scattering or reflection from the target, or from the intervening atmospheric path can also produce detector noise. This will be particularly significant for a sensitive detector system, in the visible or near visible range, where bulk of solar power arrives, and it may be desirable to limit solar radiation by a filter passing through a laser line. Sensitivity of the detector system is better in night than the day time. The total radiation from the entire sky on the earth is  $10^{-10}$  W/ cm<sup>2</sup>; and the total solar radiation on the earth is 13w/cm<sup>2</sup> , whereas the reflected radiation from the moon is approximately  $10^{-6}$  or less [24]. For a detector sensitive to CO<sub>2</sub> laser radiation, the significant background radiation will be thermal (black body) and not the scattered sunlight. It is often reduced by the proper cooling system. Laser radiation backscattered from the atmosphere is an important source of noise at short ranges.

**Other noise sources:** The signal power output coupled from the photomixing device should be greater than the noise power of succeeding amplifiers or RF mixers. If the coupling is inefficient considerable amount of signal power may be lost. Thus it is desirable to have some form of gain between the photo cathode and the output coupling. The commonly used method is secondary emission multiplication. However this can increase the noise level

#### **4.4 PULSE INTEGRATION**

Generally most range finders use only a single transmitted pulse. Signal to noise ratio can be improved by integrating many pulses. It is generally used in moon/ satellite range finders which uses high pulse repetition rate and CO<sub>2</sub> lasers and also for low power GaAs laser range finders.

#### **4.5 CHOICE OF TRANSMITTER WAVEFORM**

Transmitter waveform has to be properly chosen as per the requirements of the target of interest.

##### **4.5.1 RANGE FINDERS USING NATURAL TARGETS, PULSED SOURCES AND DIRECT DETECTION**

The optical depth of natural targets (trees, buildings, at possible oblique incidence) is in the range of a few meters. This sets a limit to the accuracy that is useful and thus sets a lower limit to useful pulse length, of order 25ns. This length of pulse fits well with those provided by Q-switched solid state lasers or gain switched gas lasers.

Even if the accuracy requirement were relaxed, there is an energy advantage in keeping to as a short a pulse as the detector will handle. This is generally useful in a receiver that detects individually photo-events (e.g. a photo multiplier ). If a weak return from random counts due to noise background etc. the photo events from the return are concentrated in to the smallest possible time interval, they will have a maximum statistical significance compared with background photo events, especially when the probability of a background event in the time interval becomes very small. For a receiver incapable of detecting individual photo events, it is advantageous to compress the available energy into the shortest pulse.

#### **4.5.2 LUNAR RANGE FINDERS USING RETRO REFLECTORS,PULSED SOURCES AND DIRECT DETECTION:**

In lunar range finders returns are weak but precision is more important. Target optical depth is now in the range of small fractions of a meter, so that pulses of order 1ns and available energy are useful. System design thus requires fast efficient, low noise detectors (High speed photo multipliers) combined with very short laser pulses in the visible region. The time available for measurement permits integration over many pulses.

#### **4.5.3 SURVEYING INSTRUMENTS USING RETRO REFLECTORS, MODULATED CW SOURCES AND DIRECT DETECTION:**

In these range finders the prime aim is accuracy. The use of retro reflectors provides not only a precise target distance, but makes signal strength a secondary problem (at least upto several km range). Measurement speed is also a secondary consideration. The precision attainable in phase measurement accurate to within 0.1% of  $2\pi$  phase at 50MHz (corresponding to 3mm range uncertainty), corresponds to a timing accuracy of 20 ps, which would clearly be difficult to attain by the direct measurement because detector response times are usually inadequate. The advantage in energy terms of long duration transmission for direct detection systems are limited hence high accuracy is obtained with modulated wave forms lasting many seconds.

#### **4.6 HETERODYNE DETECTION SYSTEMS**

In a heterodyne detection system the signal electrical power emerging from the detector is proportional to the optical signal power incident on the detector.(for direct detection the signal amplitude at detector output is proportional to incident optical power).The implications for transmitter waveform design are similar to those for micro wave radar, where heterodyne detection is the normal receiver technique: provided that the receiver has a matched filter (designed to detect optimally a weak signal with known wave form in white noise),then the detectability of the signal is determined by the signal energy, and the waveform duration and



modulation are immaterial in the optical heterodyne case. The probabilistic nature of the photo detection process makes this result only an approximation, but it is a reasonable guide for the important case of the CO<sub>2</sub> laser heterodyne receiver, where individual photo-events are not discernible .

An important difference between the optical and microwave cases is that Doppler frequencies  $f_D = 2v/\lambda$  are vastly larger in the optical case, if different parts of the target have different velocities, they cause different Doppler shifts and time dependent interference effects occur ,so that the total return wave form is different from the transmitted, and it is said to be loss of temporal coherence. So the length of the pulse should be proper value if it less than the required value, the signal processing efficiency fall off, hence there is an upper limit on pulse duration. However, if pulse duration is kept below this coherence time, there is a considerable choice of transmitter waveforms .The choice is limited by the availability of frequency stable laser sources. In practice only concerned with CO<sub>2</sub> lasers and the choice between pulses from the pulse excited TEA lasers and modulated waveforms derived from CW lasers Here the range accuracy is determined by the frequency bandwidth of the pulse. Hence higher accuracy can therefore be obtained by a long duration pulse with high bandwidth frequency modulation.

The return pulse will be Doppler shifted when the target has nonzero radial velocity. The range of moving target is obtained by the Doppler frequency shift. By use of modern signal processing techniques return with unknown Doppler shift is obtained by the proper choice of transmitted waveform. The need to cope with Doppler shifts is therefore an important factor in system design.

For an efficient signal processing, a simple un modulated pulse of duration  $\tau$  would require a bank of Doppler filters covering the range of expected Doppler shifts and each having a band width about  $1/\tau$ . For a pulse with linear frequency modulation (i.e. "chirp"pulse), obtained by modulating a CW laser, one would select a pulse as long as possible (approaching the coherence time limit) to maximize energy transmission; range accuracy would be determined by frequency swing. The major effect of Doppler shifts well below the pulse width which can be handled in a single channel (pulse compressor), is to produced a range error. If the range error is unacceptable, it is possible to determine the range and target Doppler by

combining the result from Up-chirp & down chirp transmissions (which produce errors of opposite signs.)[5]

## **4.7 LASER EYE HAZARDS**

The human eye transmits comparitily well from 450- 1150 nanometers. At 1200nm the transmission has fallen to ~10%, and beyond 1400 nm it becomes extremely small. Therefore the short wavelength lasers (Nd, GaAs, ruby, doubled-Nd) have a low eye damage threshold energies (or powers), because the radiation is focussed on the retina. For single Q-switched pulses incident on the eye, for ruby lasers it is  $5 \times 10^{-7} \text{ J cm}^{-2}$  and for neodymium lasers it is  $5 \times 10^{-6} \text{ J cm}^{-2}$ . For holmium and CO<sub>2</sub> lasers the radiation does not reach the retina and the corresponding single Q-switched – pulsed protection standard is  $1 \times 10^{-2} \text{ J cm}^{-2}$ , i.e. it is a factor of  $2 \times 10^3$  higher than for a neodymium pulse.

### **4.7.1 Eye safe systems**

Eye safe systems are very important where there is a possibility that the radiation might fall on human beings. This is especially important while using Nd:YAG based systems and GaAs systems which are popular in military applications.

## **4.8 SIGNAL AVERAGING TECHNIQUES**

These techniques are aimed at improving the signal to noise ratio simply by reducing the noise accompanying the signal. There are two basic ways of doing this.

### **4.8.1 BAND WIDTH REDUCTION**

Here the noise is reduced by reducing the system noise bandwidth (Bn). This approach works well if the frequency spectrum of the noise signal do not overlap significantly, so that reducing the bandwidth does not effect the signal. With random white noise output noise is proportional to  $\sqrt{Bn}$ .

### 4.8.2 AVERAGING OR INTEGRATING TECHNIQUE

In this technique successive samples of the signal are synchronized and added together. The signal will grow as the number (N) of added samples; while the random white noise grow as  $\sqrt{N}$ . In many applications, there is a significant overlap between the signal and noise spectra and improving a signal to noise ratio must be done at the expense of the response time, or measurement time (T). With random white noise interference the output signal to noise ratio is proportional to  $\sqrt{T}$ . The bandwidth reduction technique is best from frequency domain point of view; while signal averaging and correlation techniques are best from time domain analysis viewpoint.

The signal averaging may be either single-point or multipoint. The boxcar integrator is an example of a single point averager; where it samples each signal occurrence (sweep) only once. A multi point signal averager is like a large number of boxcars connected in parallel, since it samples many points (typically  $2^{10}=1024$ ) during each signal sweep. In this case the analog storage capacity of the boxcar is replaced by a digital memory. The incoming (input) signal is first sampled and digitized and new data are added to the data from previous sweeps already in the memory location corresponding to that sampling point. The functional block diagram of a signal averager is shown in Fig 4.1.

Basic concept of this technique is described below. First consider the typical waveforms and timing details for a multi-point averager as shown in Fig 4.2. For example if  $I=10$ , then only 10 samples or sweep are shown. The total signal duration (T) is given by the product of the number of samples or sweep (I) and the dwell time (gate width of sampling duration,  $t_g$ ) of each sample. Here T is less than the total sweep duration ( $\tau$ ) by the dead time ( $t_d$ ), and there is usually a fixed time between the receipt of a trigger pulse and the beginning of the first sample. In many applications, the multi-point averager is triggered at a constant rate ( $f=1/\tau$ ). It is not necessary that the trigger be periodic. Assume that the averager is set to continue averaging until all input sweeps have been sampled, at which point it will automatically stop. Suppose we wish to recover the wave form of a noisy signal,  $f(t)$ , where

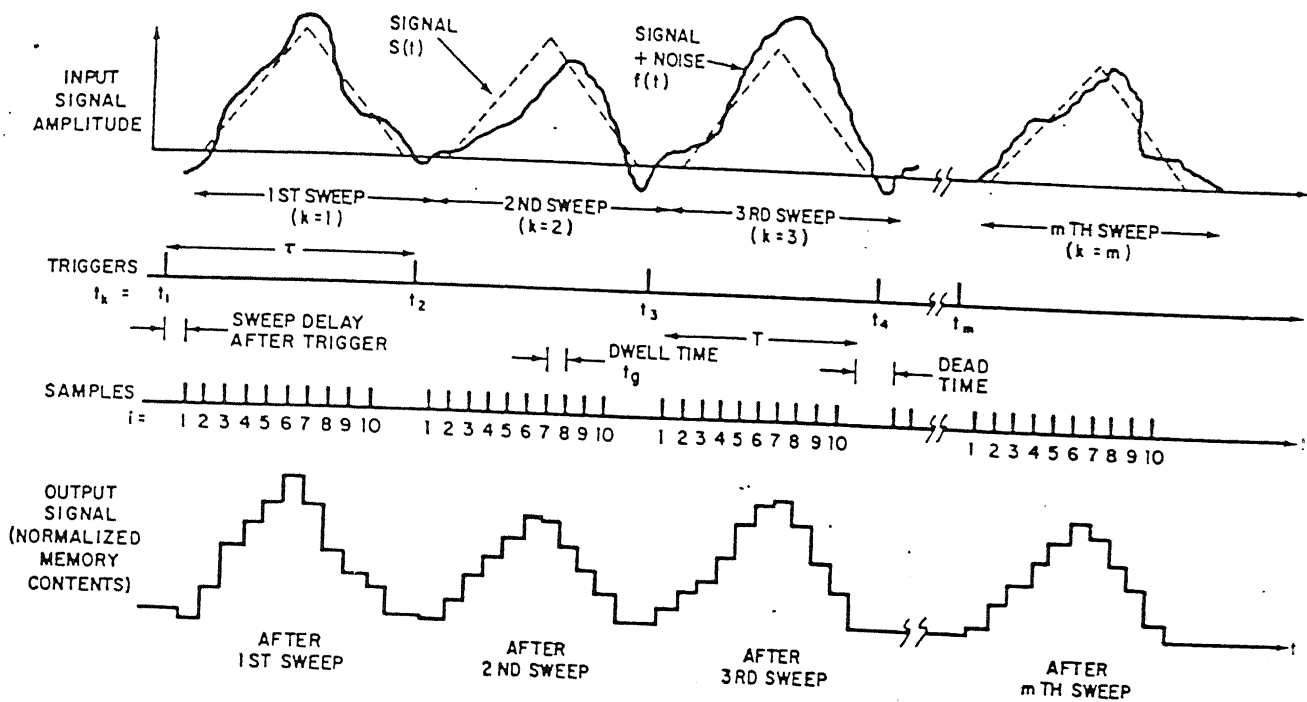


Fig 4.2: Multipoint averaging [48]

$$f(t) = s(t) + n(t) \text{-----} (4.1)$$

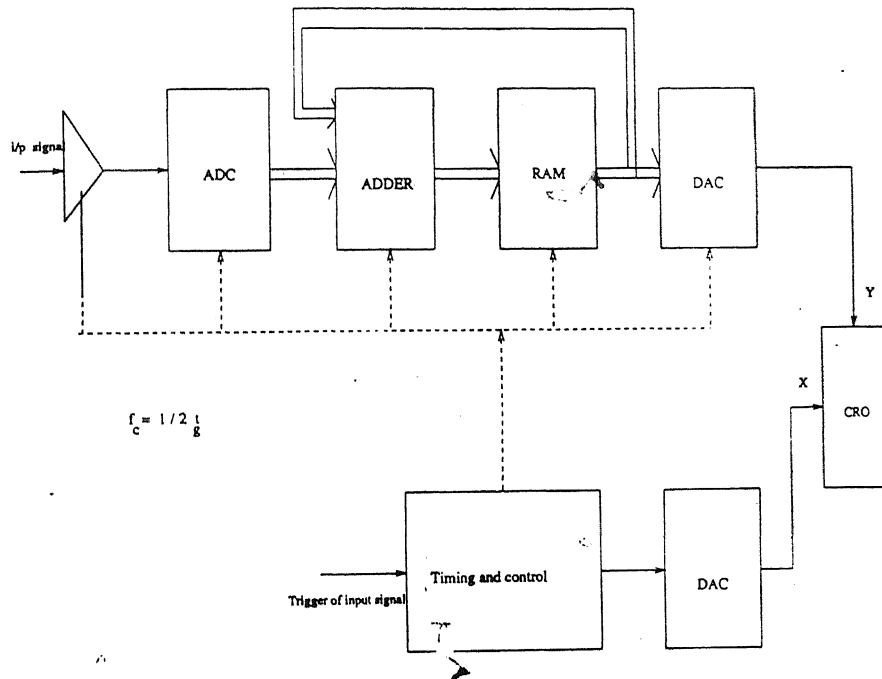


Fig4.1: Basic block diagram of a signal averager

For the  $i$ th sample of the  $k$ th sweep,

$$f(t) = f(t_k + it_g) = s(t_k + it_g) + n(t_k + it_g) \text{-----} (4.2)$$

For any particular sample point (i) the input signal can be assumed to be unchanged with each new value of  $k$  (i.e. with each new sweep) and the averaged signal will therefore be simply

$$s(i)_{out} = \sum_{k=1}^m s(t_k + it_g) = ms(it_g) \text{-----} (4.3)$$

For random noise, samples ( $X_i$ ) will add vectorially so that the r.m.s. value ( $\sigma$ ) of the average noise will be given by

$$\left( \sum (X_i)^2 \right)^{1/2} = \sigma \sqrt{m} \text{-----} (4.4)$$

The averager output can be described by

$$g(t_k + it_g) = ms(it_g) + \sigma \sqrt{m} \text{-----} (4.5)$$

so that the output SNR is

$$SNR_{out} = \frac{S_{out}}{N_{out}} = \frac{ms}{\sigma \sqrt{m}} it_g = \frac{s}{\sigma} it_g \sqrt{m} \text{-----} (4.6)$$

The input SNR is simply

$$SNR_{in} = s(it_g) / \sigma \text{-----} (4.7)$$

so that the SNR improvement is given by

$$SNIR = \frac{SNR_{out}}{SNR_{in}} = \sqrt{m} \text{-----} (4.8)$$

When we see the response of multi-point averager, linear summation mode of averaging has been assumed. That is, for the  $i$ th memory location, the average after  $m$  sweep is given by

$$A_m = \sum_{k=1}^m f(t_k + it_g) = \sum_{k=1}^m I_k \text{-----} (4.9)$$

where  $I_k = f(t_k + it_g)$  is the value of the  $i$ th sample in the  $k$ th sweep.

During each sweep the data ( $A_{k-1}$ ) in each memory location are compared with the new sample value  $I_k$  and the computed value of the  $(I_k - A_{k-1})/k$  is added to memory to form the new average value  $A_k$ . Because of practical difficulties in implementing a division by  $k$  during or after each sweep, the algorithm shown in the equation (4.10) can be approximated as

$$A_k = \frac{1}{k} \sum_{k=1}^m I_k = A_{k-1} + \frac{I_k - A_{k-1}}{k} \text{-----} (4.10)$$

$$A_k = A_{k-1} + \frac{I_k - A_{k-1}}{2^J} \text{-----} (4.11)$$

Where  $J$  is a positive integer selected automatically such that  $2^J$  is the closest approximation to  $k$ . By proper selection of  $J$  value the noise signal shrinks with time, Hence it provides a stable constant amplitude display; the larger the value of  $J$  selected, the greater the signal enhancement and more slowly the average response to the change in the input signal. For large number of sweeps, SNIR is given by

$$SNIR \approx \sqrt{2^{J+1}} \text{-----} (4.12)$$

## CHAPTER 5

### HARDWARE IMPLEMENTATION OF LASER RANGE FINDER SUBSYSTEMS

An attempt has been made to implement some subsystems of a laser range finder, viz. transmitter, receiver, and digital signal averager. These subsystems are briefly described below.

#### 5.1 HARDWARE IMPLEMENTATION OF A DIGITAL SIGNAL AVERAGER

The function of this subsystem is to collect the successive samples of the signal, synchronize them and add them together. The signal will grow as the number  $N$  of the added samples; with the random white noise the noise growing as  $\sqrt{N}$ .

The main experimental part of the study has been aimed at designing and testing a suitable Digital signal averager scheme with the available hardware. The basic block diagram of the implemented signal averager is shown in Fig.5.1. The input signal to the analog-to-digital converter (ADC) which is coming from the receiver is embedded with noise. In order to extract the signal from noise a form of pulse integration technique is used. Here signal characteristics are deterministic (repetitive) while the noise is random. If the large number of data samples are averaged, the random noise will average to zero, while the repetitive signal will converge to its mean value. Here instead of averaging the signal, the signal and noise were summed together. Hence the noise will add up to a certain value instead of the noise averaging to zero.

The input signal is first sampled, digitized and stored in the (RAM) memory, bin after bin. We considered the signal over 256 bins (or digital windows), with bin 0



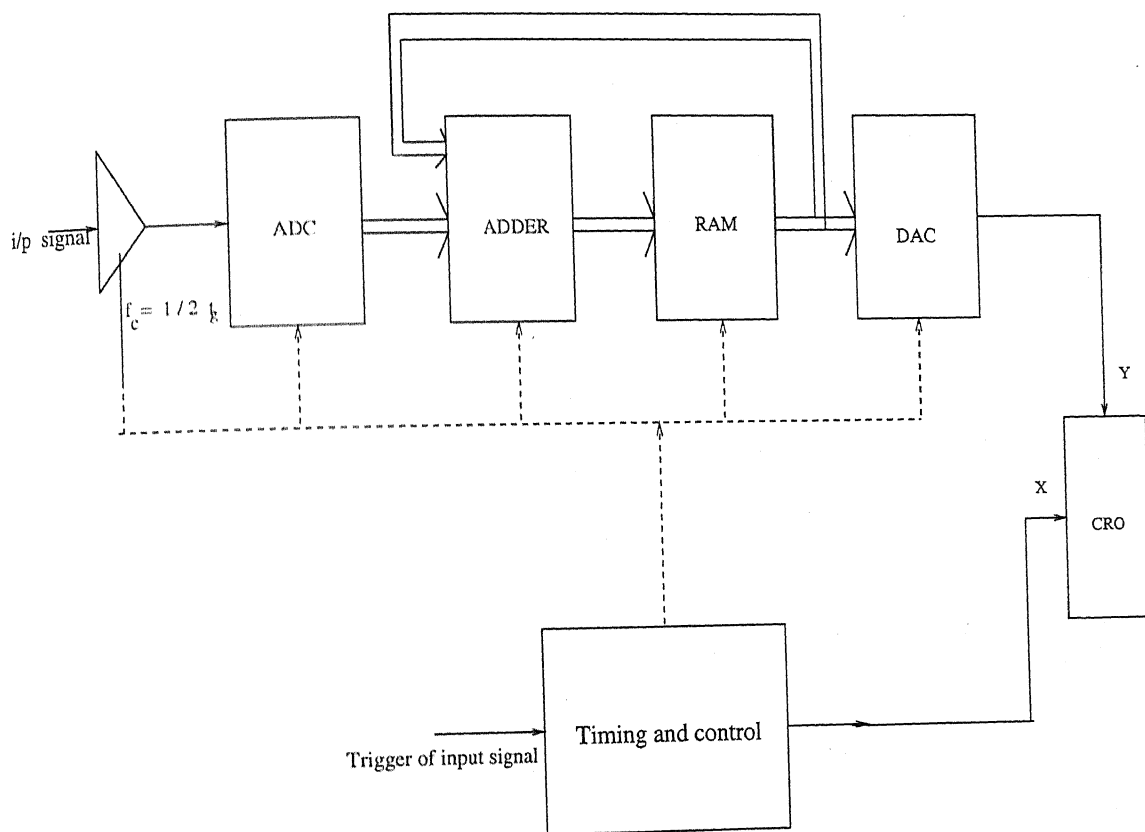


Fig 5.1: The Basic Block diagram of the implemented Signal Averager.



corresponding to the time frame of the transmitted pulse and bin 255 to the farthest target. A special timing circuitry was designed to ensure proper synchronization of the various bins. The signal corresponding to each bin was presented to the ADC and its output was added to the previous data stored in the RAM. This new value was then presented to a digital-to-analog converter (DAC) and also stored in the location of RAM corresponding to that bin. The DAC output was displayed on a CRO. With proper external triggering of the oscilloscope the CRO displays all the bins from 0 to 255. It was expected that in N such scans, each scan covering bins 0 to 255, the noise would settle to a certain mean value while the wanted signal will add up and will be seen prominently in the display. In order to maintain proper synchronization at all the stages of the signal averager, proper timing and control circuit must be done. The main circuit of the above scheme is shown in Fig.5.2.

### 5.1.1 SYSTEM TIMING AND CONTROL SIGNAL GENERATORS

This is one of the most crucial part of the signal averager and hence care should be taken in the design and implementation of this block. The timing and control signal generator is based on a few counters, which keep track of the current bin and its timing. Block schematics of these counters is shown in Fig.5.3.

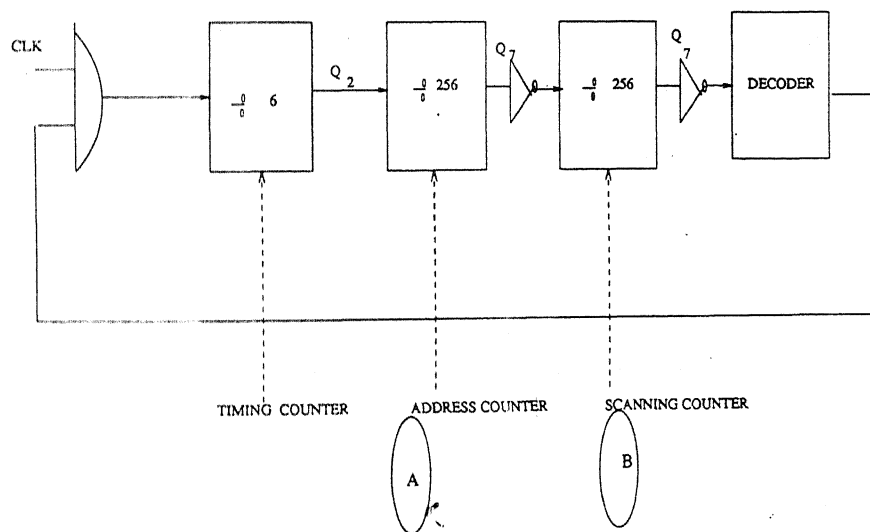


Fig.5.3 Block diagram of the main counters

The basic counter in the above counter chain is the mod-6 (divide-by-six) counter. This counter is designed as a cascade of mod-3 and mod-2 for simplicity and was implemented using three, 74S112 dual negative edge triggered JK-flip-flops. Circuit diagram of this counter is shown in Fig. 5.4. As a result of the above cascading the six sequence of states of the counter are ( $Q_2 Q_1 Q_0$ ): 000, 001, 010, 100, 101, and 110, where  $Q_2$  is the MSB and  $Q_0$  is the LSB. The operation in each bin, such as digitizing the signal, adding the samples, storing the added value in the RAM and outputting the latest bin value to the DAC, were all derived by decoding individual states of this counter. These are explained in later sections. The main bottle-neck in the whole averager had been the ADC which had a typical conversion time of 15-18 $\mu$ s. The timing diagram of the ADC used in our scheme is shown in Fig. 5.5. The main signals of the ADC are  $\overline{CS}$ ,  $\overline{RD}$  and  $\overline{BUSY}$ , where the first two are input control signals and the third one a status output. The ADC starts digitizing with  $\overline{CS}=0$  and  $\overline{RD}=1$ , which is called the 'Convert cycle of the ADC'. This is indicated by a '0' level on the  $\overline{BUSY}$  output of the ADC. Once the conversion is over the contents of the ADC registers may be read by issuing  $\overline{CS}=0$  and  $\overline{RD}=0$ . This is termed the 'Read cycle of the ADC'. It is important that the read cycle is initiated only after the  $\overline{BUSY}$  output goes HIGH, thereby indicating that the conversion is over. This was ensured by choosing an input clock (CLK) frequency of 200 kHz (i.e a period of 5 $\mu$ s) for the mod-6 counter and deriving the read cycle signals from the counter well after the conversion period. With the above clock frequency the total time for available per bin was 30 $\mu$ s (=6X5 $\mu$ s). Out of this 25 $\mu$ s was reserved for the ADC and the remaining 5 $\mu$ s for all the other operations put together.

The control signals for the ADC as shown in Fig. 5.6: and it is generated by the mod-6 counter as shown in Fig 5.6. Timing sequence of the ADC control signals are shown in Fig. 5.7. As seen in Fig. 5.6, the two  $\overline{CS}$  signals for the ADC, one for the convert cycle and one for the read cycle, are decoded using 7410 3-input NAND gates. These two decoded signals are combined using a 7408 AND gate which is applied to the

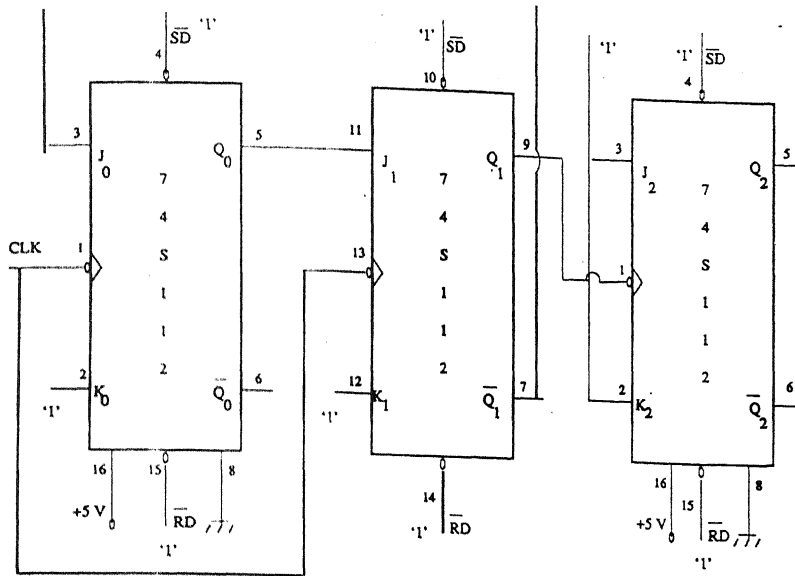


Fig. 5.4 Basic timing circuit (Mod-6 Counter)

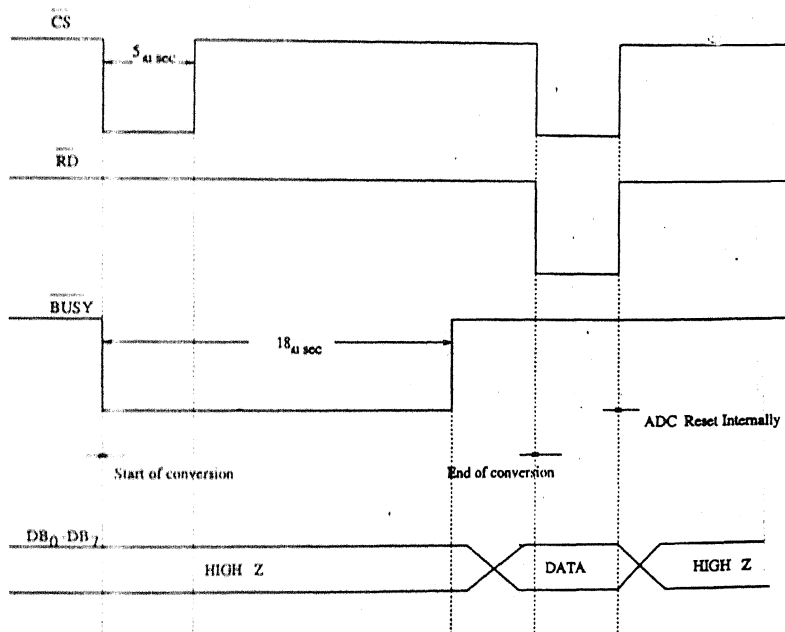


Fig.5.5 Timing diagram of AD7574 ADC

$\overline{CS}$  pin of the ADC. The relative timing of the  $\overline{BUSY}$  with respect to the ADC control signals is indicated in Fig.5.7.

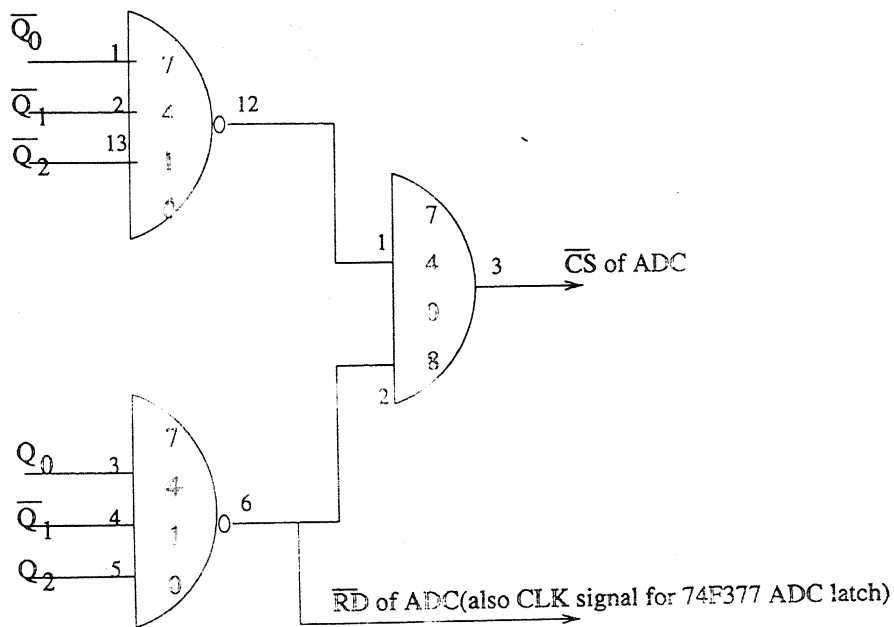


Fig.5.6 Decoding of the ADC timing signals

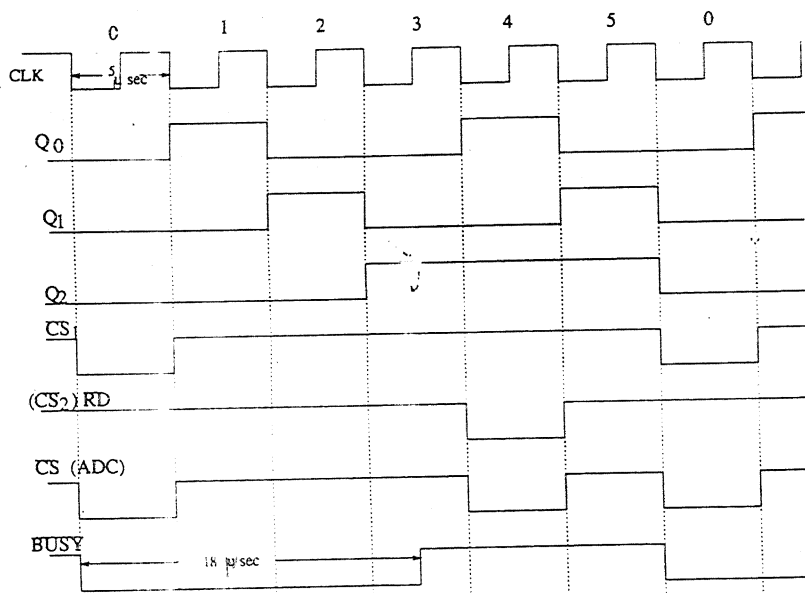


Fig.5.7 Timing sequence of ADC signals

### 5.1.2 AD7574 ADC AND ADDER

In the signal averaging design, the input signal coming from the receiver is fed to the analog input terminals of the ADC. The ADC is used in our work was AD7574. It has two input control signals  $\overline{CS}$  and  $\overline{RD}$  (Chip Select & Read). The chip select is decoded device address. These two inputs control all ADC operations such as starting of conversion and reading the data. The ADC output data bits use three state logic, allowing the direct connection to microprocessor data bus and system bus. In our case the ADC outputs were fed to an adder. Decoded timing signals of  $\overline{CS}$  and  $\overline{RD}$  were shown in Fig.5.7. When the timing sequence of  $\overline{CS}$  and  $\overline{RD}$  are proper, the ADC will automatically generate  $\overline{BUSY}$  (output) signal. The truth table of ADC interface with RAM as shown.  $\overline{BUSY}$  must be HIGH before a data read is attempted: i.e. the total delay between a convert start and data read must be atleast as great as the AD7574 conversion time (typically 15 $\mu$ s). Once  $\overline{BUSY}$  signal goes HIGH conversion is completed. If  $\overline{RD}$  goes from LOW to HIGH, when  $\overline{CS}$  is LOW, the ADC is internally reset and the ADC data is lost. Hence, before,  $\overline{RD}$  goes from LOW to HIGH the data (output of ADC) should be collected in a 8-bit latch. We used a 74F377 8-bit latch for this purpose which used the  $\overline{RD}$  signal of ADC as a clock signal. 74F377 is a fast logic octal D Flip-flop with enable input and tri-state control.

The AD7574 has an internal asynchronous clock oscillator, which starts upon the receipt of start-convert command and cease oscillation when conversion is complete. It requires an external R and C components for a nominal conversion time of 15 $\mu$ s. R, C used were R=120K, C=100pF. AD7574 can be operated in both unipolar and bipolar modes. For unipolar operation the supply voltage is +5V and  $V_{ref}$  is -10V. For best results is necessary to adjust the gain and offset control.

The data output (ADC output)  $DB_0$  to  $DB_7$  were connected through the 8-bit latch, to the 'A'-inputs of a 8-bit Adder, obtained by cascading two 4-bit adders, 74LS83. The other set of inputs of the adder ('B' inputs) are taken from the output of the RAM. The 8

bit output of the adder is first loaded into another 8-bit octal latch (74F377) and then connected to a tri-state octal buffer (74244). The clock signal for octal latch at the adder output is the complement of the  $\overline{WR}$  signal used for the RAM, while the  $\overline{OE}$  (output enable) input for the tri-state buffer is the same as  $\overline{WR}$ . Generation of  $\overline{WR}$  and other RAM signals are explained later. The output of the adder through the octal latch and tri-state buffer is connected both to the RAM data input and the DAC input.

### **5.1.3 STORING OF ADDED DATA IN MEMORY (RAM)**

For our study we used the 6116, 2K x 8bit RAM. This RAM has 11 address lines ( $A_0$ - $A_{11}$ ) and 8 data lines ( $D_0$ - $D_7$ ). This IC is specified to have a total access time of 120ns and an output enable access time of 50ns. Even though 2K capacity was much more than what we needed, this RAM was used as it was readily available and had very low access times. The three signals controlling the various functions of this chip are  $\overline{RD}$ ,  $\overline{CS}$  and  $\overline{WR}$ . When  $\overline{WR}$  and  $\overline{CS}$  are LOW it is in write mode, while when  $\overline{CS}$  and  $\overline{RD}$  are LOW it is in read mode. In our application we kept  $\overline{CS}$  permanently LOW. The data from the adder was written into the RAM when  $\overline{WR}$  of the RAM is LOW, which occurred during the last state of the mod-6 counter. As explained earlier  $\overline{WR}$  signal is used in both the latch and buffer leading to the Ram, thereby ensuring that data for writing into the RAM from the adder is available during every  $\overline{WR}$  signal. The RAM was put into read mode during the earlier states of the mod-6 counter, thereby ensuring that the B inputs of the adder have data ready when the data from the ADC is latched to the A inputs. It was necessary to hold the read data from the RAM in a register, for which purpose another 74F377 octal latch was utilized, whose outputs were fed to the B input of the adder. This type of parallel operation enabled speeding up the averaging process. The detailed timing These are decoded from the timing and control signal generator. The timing sequence of the RAM control signals is shown in Fig.5.8. Derivation of the control signals for the RAM, latches and tri-state buffer is as follows.



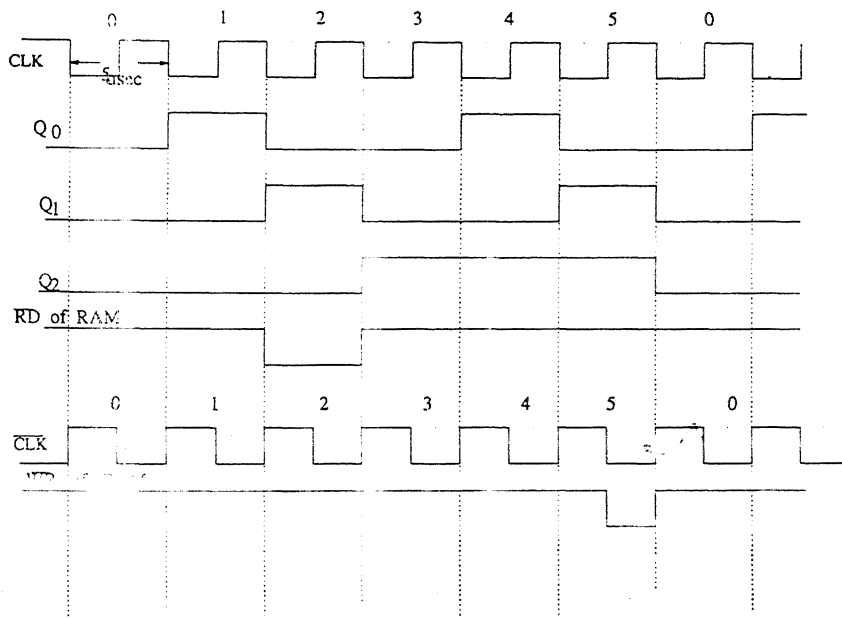


Fig. 5.8: Timing sequence of RAM

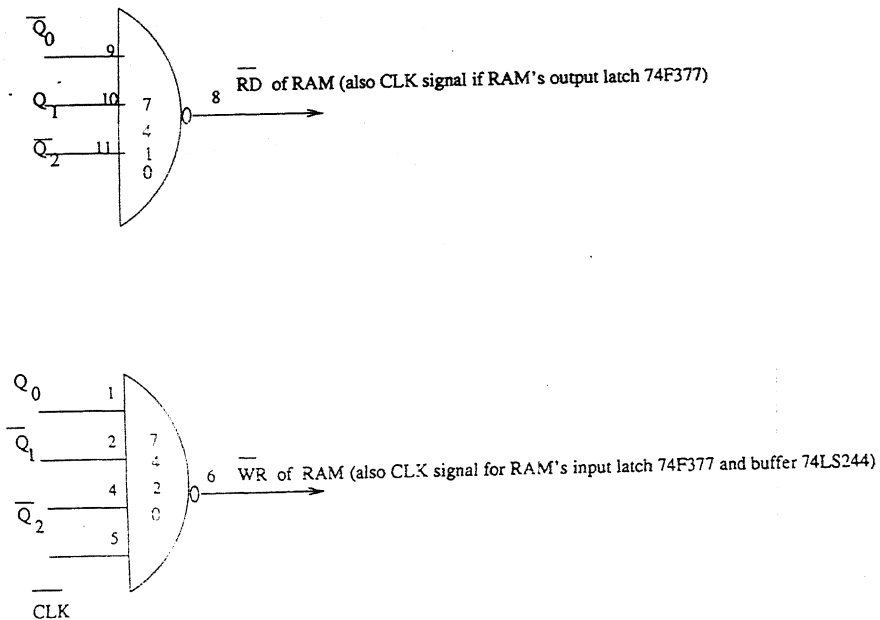


Fig.5.9 Generation of  $\overline{RD}$  and  $\overline{WR}$  signals for RAM

The  $\overline{WR}$  signal of RAM is decoded using a 7420 4-input NAND gate where a half cycle delay is provided using the clock because the data requires some settling time before it is written into the RAM.  $\overline{RD}$  signal is decoded using a 7410 3-input NAND gate decoder. Each read and write operation should be done at the RAM location corresponding to the bin in question. For this purpose 8 bit counter was used which used the output of the MSB output of the mod-6 counter as the clock. This ensured bin addresses selections from 0 to 255 for each read and write operation. One, In order to reset the RAM one way is switch of the power supply, other way is to load zero's in all memory locations. This logic used for the generation of  $\overline{RD}$  and  $\overline{WR}$  signals is shown in Fig.5.9. In summary, the main data operations involving the RAM in every bin period are

1. Reading the old data from RAM to the 'B' inputs of the adder
2. Latching the data from ADC to the 'A' inputs of the adder
3. Adding of the data
4. Writing the added data of the current bin into RAM
5. Display the RAM contents on CRO
6. Get ready for the next bin

When all the above operations are over, one cycle will be completed.

#### **5.1.4 CONVERSION OF DIGITAL DATA TO ANALOG SIGNAL AND DISPLAY**

The main element involved in displaying signal on a CRO is the DAC. AD558 DAC was used in our study which was a microprocessor-compatible 8-bit digital to analog counter. The output of DAC is available in one of the two voltages are ranges, viz. 0-2.5v range or 0-10v range. Correspondingly, the supply voltages required are 5V and 15V, respectively. This DAC has fast settling time and has an internal output amplifier and a precision voltage reference on a single monolithic chip. No external components or trims are required to interface with full accuracy from an 8-bit data bus to an analog system. The reference voltage is -10 volts. In our case, the data inputs (Do-D<sub>7</sub>) were

connected from the 8-bit adder outputs through an 8-bit latch and the tri-state buffer. The DAC converts the TTL level digital inputs into the corresponding analog output. It has two control signals, viz.  $\overline{CS}$  and  $\overline{CE}$ , corresponding to chip select and chip enable, respectively. In our case since the DAC inputs were connected to the latched outputs of RAM and hence the  $\overline{CS}$  and  $\overline{CE}$  inputs were permanently enabled by making them LOW. The output of the DAC was directly connected to the CRO.

### **5.1.5 SELECTION OF ADDRESS LINES (ADDRESS COUNTER)**

An 8-bit address counter was used which provided the correct bin address during each cycle. 74F779 IC was used for this purpose which had 8-bit synchronous UP/DOWN counter built in a single chip and had a maximum operating frequency of 145 MHz with a typical supply current of 90 mA. This counter outputs were connected to the address lines of 6116 RAM. The input clock signal for this counter came from the MSB ( $Q_2$  output) of the mod-6 timing and control generator. For each positive going edge of the clock the counter will increment in binary form from 0 to 255. Count up operation was required in our case and hence the control signals are set as follows; S1 input -HIGH, S0 input -LOW, and  $\overline{CE}$  -LOW. Timing diagram of this counter is shown in Fig 5.10.

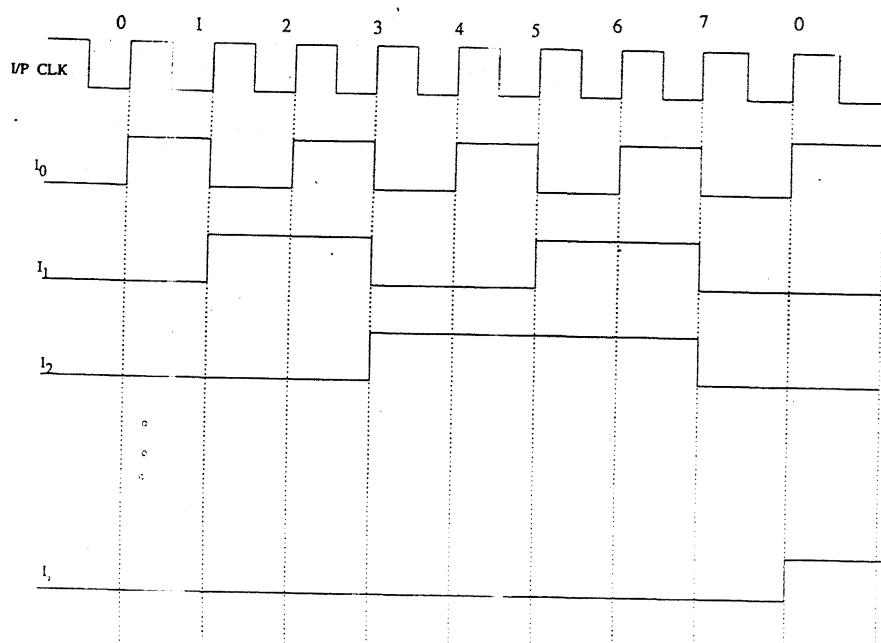


Fig.5.10:Timing sequence of the address counter

### 5.1.6 CONTROLLING OF NO OF SCANS (SCANNING COUNTER)

The main aim of the implemented signal averager was to improve the signal-to-noise ratio by increasing the number of measurement scans,  $N$ . Hence it is important to have a facility to control  $N$ . This was implemented in our system using a scan counter, which could keep track of scans up to 255. The measurement cycles could stopped after a given number of scans  $N$ , by decoding  $N$  at the scan counter outs and stopping further input acquisition and data processing. Detailed circuit diagram of the scan counter implementation is shown in Fig.5.11. Our 8-bit counter was implemented using two 4-bit synchronous counters, 74161 ICs, which had asynchronous clear facility. The clock input to this counter is obtained from the  $Q_7$  output of the address counter ( $\overline{Q_7}$  is used as the clock of the scan counter to ensure that the scan counts are updated at the end of every scan. For each positive going clock edge  $\overline{Q_7}$  the counter will increment from 0 to 255. The required number of scans,  $N$ , was decoded using an 8-input NAND gate (7430). Thus it was possible to choose any value of  $N$  from 1 to 255. In our case measurements were taken for  $N=127$ . To disable the averaging of data and storing them beyond  $N$ , a special circuitry was made using 74S112 JK flip-flop and 7432 2-input OR gate. The JK flip-flop was initially cleared by making the input  $\overline{CLR} = \text{LOW}$ . The  $\overline{WR}$  signal applied to the RAM was routed through the 7432 OR gate ensuring normal write operations till up to the specified  $N$ . Once the number of scans equals  $N$ , the decoder output which is used as the clock for the flip-flop sets it thereby making  $\overline{WR} = \text{HIGH}$ . This disables any further writes to the RAM. However, the DAC circuit which gets its input from the read outputs of the RAM is not affected as the read operations of the RAM are not disturbed. Normal scanning of data can be restarted by clearing the above 74S112 flip-flop and the scan counter.

We also incorporated a scan counter using 74F779 8-bit counter, which had the advantage that 8-bit operation was possible using a single chip. However, this IC had no asynchronous clear facility. Hence it was not possible to clear its contents, if rescanning of received signal is desired.



Fig 5.11: Detailed Circuit Diagram of Scan Counter Implementation

## 5.2 INPUT SIGNAL GENERATION

As mentioned earlier, it was not possible to test the signal averager using real echo signals from targets. Hence in order to test the signal averaging scheme it was necessary to generate signals which resembled typical target signals. For this purpose a few states of the RAM address counter were decoded as shown in Fig 5.12. The input signal used had a nominal width of about  $120\mu\text{s}$ , corresponding to four bin periods. For convenience bin periods 124-127 were decoded, differentiated, and suitably attenuated before applying to the ADC input. A small capacitor was put at the emitter follower output to reduce spikes before applying to the ADC. Decoding was done using 7430 8-input NAND gate. In order to see the DAC output clearly on a CRO, i.e to display signal corresponding to bin 0 at the extreme left, Q7 output of the address counter was used as the external trigger for the CRO. With our hardware implementation, signal build up was observed on the CRO at the locations corresponding to the bins mentioned above.

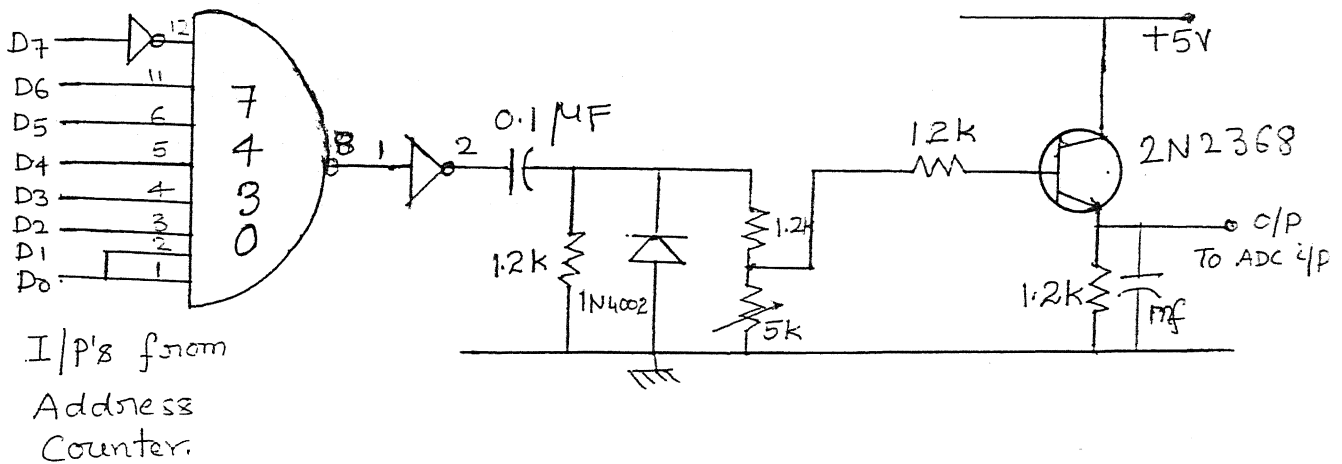


Fig.5.12 Generation of input signal

### 5.3 CLEARING THE RAM DATA

Sometimes it is necessary to clear the RAM, because if the signal and background pickup and other noise keep adding up after many scans the RAM data will be erroneous due to addition beyond the maximum upper limit (in this case 255 units). Also, at times it is necessary to clear the RAM data and start acquiring new data. A crude way of achieving this is to switch off the supply to the RAM for some period which would destroy the stored contents. However, there is no guarantee that when power is applied back to the 6116 static RAM all the memory locations are cleared. Hence a special RAM clearing circuit was designed, which is shown in Fig.5.13. Here two tri-state buffers are connected in parallel, one buffer carrying the actual data (output of adder through latch.) and the other with all inputs wired to LOW. At a time only one of the above buffers gets selected. The selection logic was controlled by a flip-flop (74S112) and logic gates (7432). The 7432 OR gates receive  $\overline{WR}$  signals at one input and HIGH or LOW, at the other input depending on the state of the flip-flop. In the normal mode,  $\overline{PR}$ =LOW,  $\overline{CLR}$ =HIGH. This will force the buffer with all LOW at its inputs to be in tri-state, while the other buffer will be able to pass the latched adder outputs to the RAM inputs. When the RAM is to be cleared, by changing the manual switch position, the flip-flop output is cleared, i.e.  $\overline{PR}$ =HIGH and  $\overline{CLR}$ =LOW. This will block normal data and pass on all zeroes the inputs of RAM, thus clearing the RAM. Normal operation is restored by changing the switch position back to the original one, i.e.  $\overline{PR}$ =LOW,  $\overline{CLR}$ =HIGH.

### 5.4 HARDWARE IMPLEMENTATION OF SUBSECTIONS (TRANSMITTER AND RECEIVER)

While designing a laser range finder the design of transmitter (laser source) and receiver plays an important role. A particular choice is based on many factors, which were discussed earlier.

Our system assumed a GaAs semiconductor laser diode as the source and a silicon device (PIN/APD) as the detector. Since the laser diode will be used in pulsed mode we thought

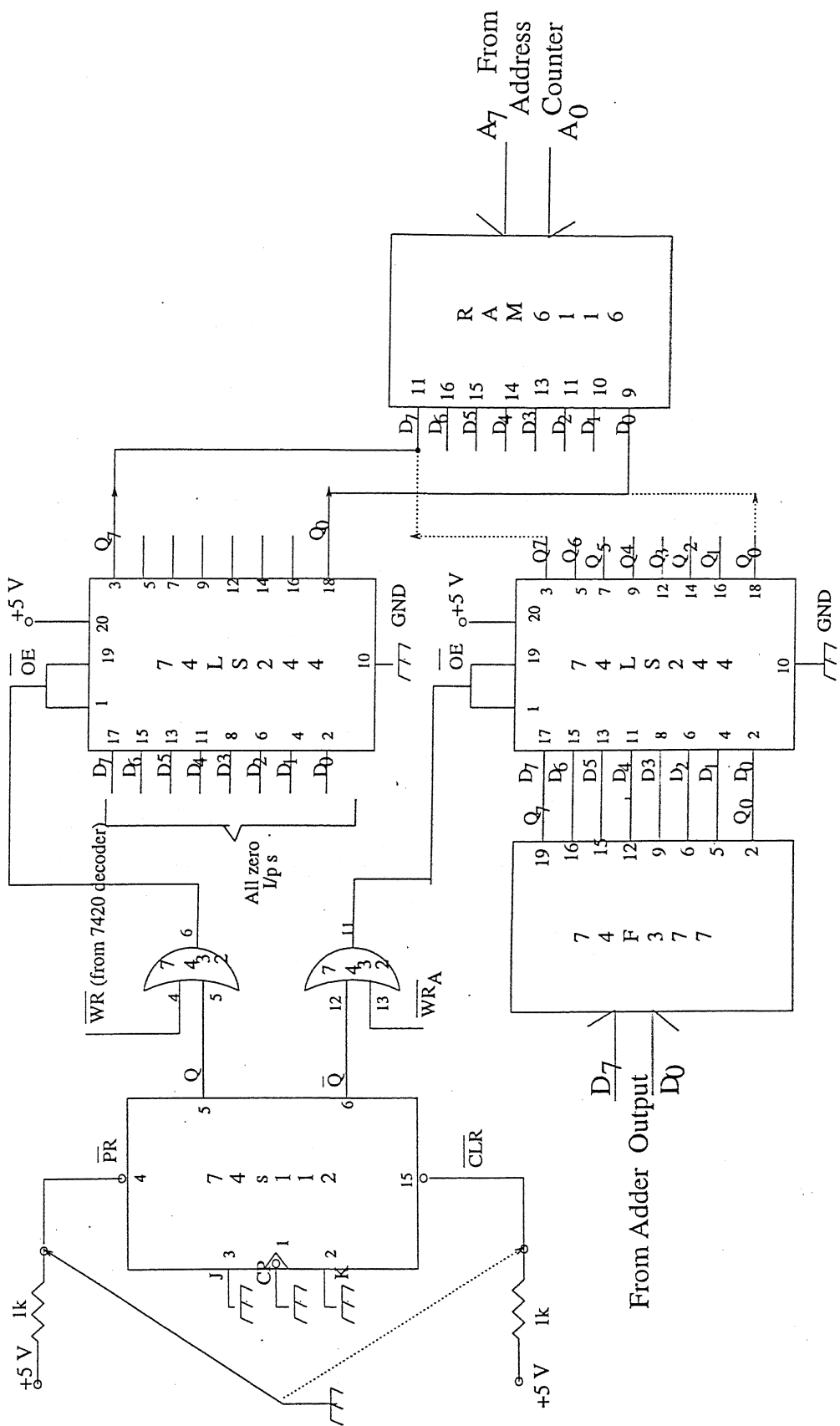


Fig 5.13 Circuit Diagram of Clearing the RAM data



of using a simple circuit making use of TTL line drivers (74S140). The current through a laser diode has two components, a fixed bias current ( $I_{\text{bias}}$ ) and a varying modulation current ( $I_{\text{mod}}$ ).

The proper selection of drive circuit is important to be able to modulate the laser with short length pulses. In order to minimize the turn-on delay it is important to keep the dc bias current close to the lasing threshold of the device. A simple optical transmitter using a LED (light emitting diode) as the source is shown Fig.5.14. It is possible to modify the above circuit for laser diode applications by connecting a suitable resistor from the cathode to ground. This would ensure a constant bias current through the device. Laser transmitter was not implemented in our study. The drive circuit of Fig.5.14 is designed by using TTL NAND drivers (74S140). It consists of two 4-input NAND drivers, each capable of supplying a current of 40 mA to the LED. By the parallel connection shown in the figure it was possible to drive 80mA of ON current through the LED. The LED used in our circuit is Motorola MFOE71. It has a specified power output of 3.5 mW at a driving current of about 100mA. Maximum forward voltage of the device was 1.8 V and its emission wavelength 820 nm.

The above transmitter output was fed to a PIN photodiode based receiver shown in Fig. 5.15. It is a simple transimpedance amplifier using TL081 BIFET OPAMP. This opamp had a gain-bandwidth product of 5MHz. Depending on the output level and also response requirement the feedback resistor can be changed. A typical value of 15K was used in our case. The PIN photodiode used was Motorola MFOD71, which had a responsivity of 0.2A/W at 820nm. The above receiver circuit along with the LED transmitter worked up to 1MHz.

A different receiver circuit shown in Fig.5.16 was also implemented and tested. This circuit was used in an earlier work [53] and it used a JFET input stage to reduce noise. The LED transmitter circuit along with this receiver circuit were capable of transmitting square pulses up to 5 MHz.

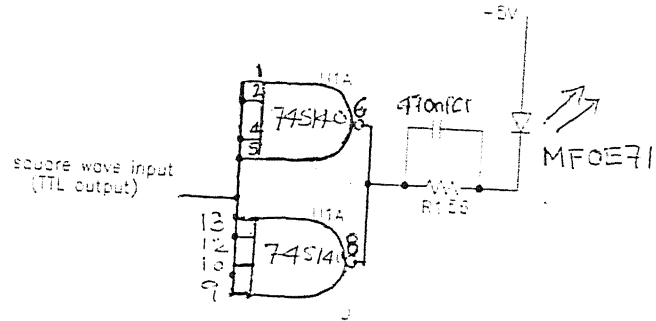


Fig.5.14 LED transmitter circuit

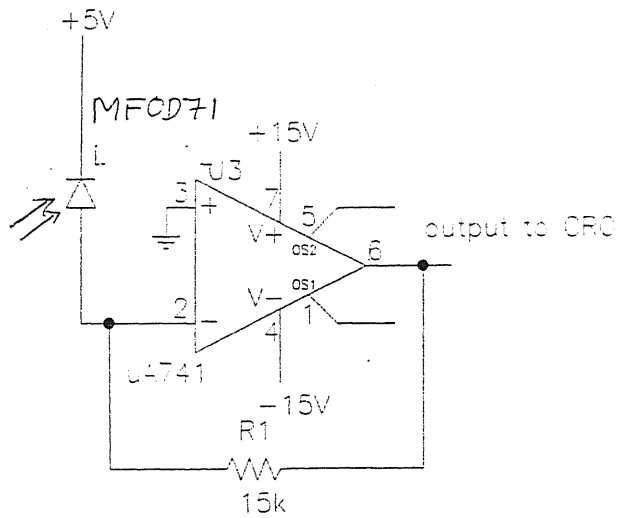


Fig.5.15 Simple receiver circuit using PIN photodiode

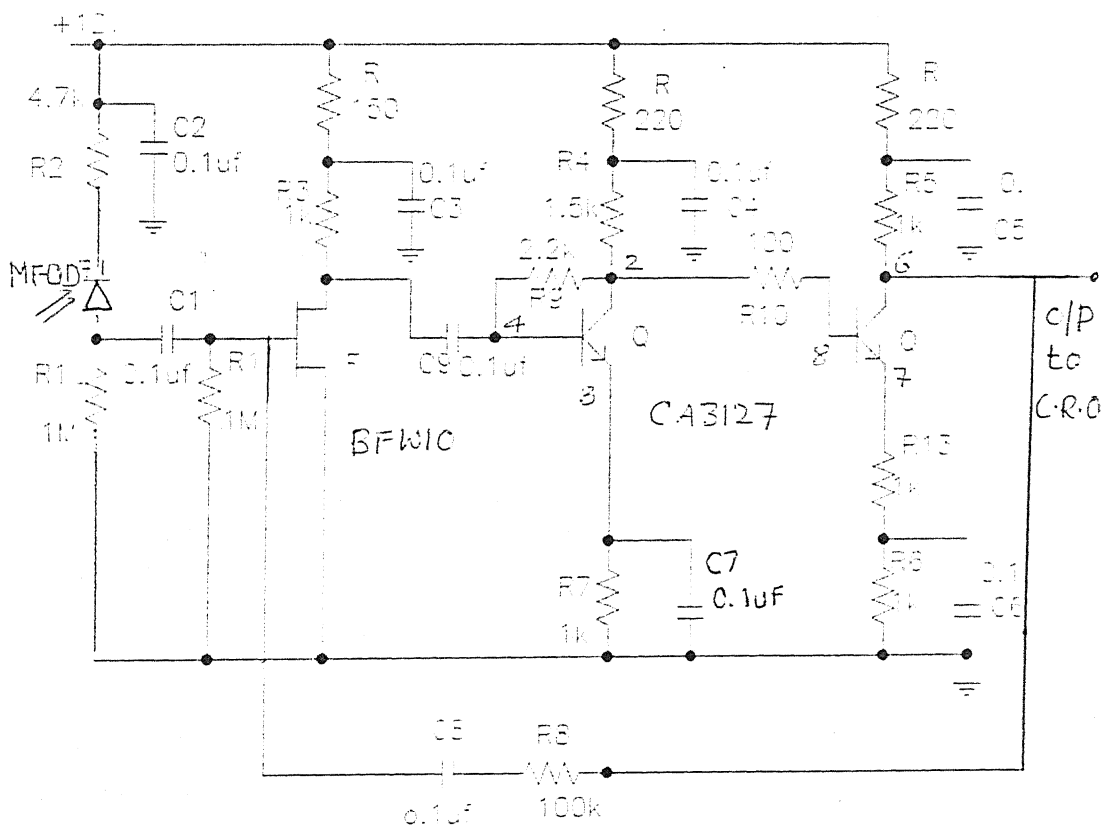


Fig.5.16 PIN receiver with JFET input stage

## CHAPTER 6

### DISCUSSION OF RESULTS, CONCLUSIONS AND SUGGESTION FOR FUTURE WORK

The main objective of the thesis was to study commonly used laser range finders and to design a suitable signal averager for an optical range finder. Detailed study of the almost all the popular laser range finders reported till date was carried out. It was found that there is no single laser finder which satisfy all the requirements of range, power, eye safety etc. Depending on the application in mind a suitable system has to be chosen and then optimised.

Eye safety is a major consideration these days. Unfortunately some of the compact laser range finders, such as the Nd:YAG and GaAs lasers have to be used with a lot of care as they emit wavelengths which falls within the sensitive range of the retina. The best option in such cases is to reduce the optical power output to meet the safety requirements and to increase the ever increasing demands for range and resolution by modern signal processing techniques.

A digital signal averaging technique was studied and the feasibility of such schemes was explored by implementing it using commonly available hardware. The ADC used in the study had a best conversion time of  $15\mu\text{s}$ , which was too large for any useful laser ranging application. However, the aim of the study has been to come up with a practical scheme of signal averaging which could be implemented. ADCs with conversion times less than  $15\mu\text{s}$  are very expensive. If fast ADCs are available the averaging technique studied could be tested with real ranging signals. The total time taken by the blocks other than the ADC was  $<1\mu\text{s}$ .

The signal improvement observable on the CRO was not as expected. This is due to the fact that the hardware implementation of the signal averaging scheme was quite complex involving several SSI, MSI and LSI chips. The noise picked up by the different parts of the averager resulted in some unexpected noise samples, which were clearly visible on the CRO.

### **SUGGESTIONS FOR FUTURE WORK**

Any further improvement to the averager scheme studied as part of the present work will involve extensive hardware. This hardware approach though faster has the disadvantage that it is inflexible and a small change to the scheme needs many hardware changes. At present several fast signal processors (Intel and Motorola families) are available, with clock rates in excess of 30MHz. Such processors are sold by both Intel and Motorola with evaluation modules which are equipped with some monitor program and some facility for interfacing. It is suggested that the signal averaging scheme should be implemented using such signal processor ICs for exploiting the speed and flexibility.

One of the major subsystems which was not studied adequately was the optics associated with the transmitter and receiver of range finders. These days GaAs visible-laser diodes are available with optical powers (CW) in excess of 5mW, but costing about Rs.100/-. With the help of suitable collimating optics GaAs based visible-laser diode range finders can be implemented.

## REFERENCES

1. Forrester P.A., Hulme K.F. "Review Laser and Range finders" *Optical Quantum Electronics*, Vol 13.(1981), pp. 259-295.
2. Walter Koechner, "Optical Ranging System Employing a High Power Injection Laser Diode" *IEEE Transaction on Aerospace and Electronic Systems*, Vol.AES-4, No.1 Jan.1968, pp.81-91.
3. Goldstein B.S., Dalrymple G.F. "Gallium Arsenide Injection Laser Radar" *Proceedings of the IEEE*, Vol. 55, No.2, Feb. 1967, pp.181-188.
4. Salathe.R., Bolleter.W, and Gilgen .H., "Long Range Injection Laser Radar" *Applied Optics*, Vol. 16, No.10, Oct. 1977, pp.2621-2623.
5. Hulme K.F., et al., "A CO<sub>2</sub> laser Range Finder using Heterodyne Detection and Chirp Pulse Compression", *Optical and Quantum Electronics*, Vol. 13, 1981, pp.35-45.
6. Takeichi.M, et al., "Streak- Camera-based Long – Distance Range Finder with 10<sup>-7</sup> Resolution" *Applied Optics*, Vol.33, No.13, May 1994, pp.2502-2509.
7. Thomas J.Kane, et al., "Coherent Laser Radar at 1.06μm using Nd:YAG Lasers", *Optics Letters*, Vol.12, No.4, April 1987, pp. 239-241.
8. Hisao Kikuta,Koichi Iwata,Ryo Nagata "Distance Measurment by the Wavelength Shift of Laser Diode Light". *Applied Optics*, Vol. 25, No.17, September 1986, pp. 2976 –2980 .
- 9.. Glenn Beheim, Klaus Fritsch "Range Finding using Frequency –Modulated Laser Diode" *Applied Optics*, Vol.25, No.9, May 1986, pp. 1439-1442.
10. Shigenobu Shinohara, et al., "Comapact and High- Precision Range Finder with Wide Dynamic Range and its Application ", *IEEE Transctions on Instrumentation and Measurment*, Vol 41, No.1, Feb. 1992, pp.40-44.
11. P.L. Bender, "Laser Measurements of Long Distances", *Proceedings of the IEEE*, Vol .55, No.6, June 1967, pp.1039-1044.
12. Bojan Turko " A Picosecond Resolution Time Digitizer for Laser Ranging", *IEEE Transactions on Nuclear Science*, Vol NS-25, No.1, Feb1978, pp.75-80.

13. Markku Koskinen, Juha Kostamovaara "An Averaging Mode Time-to-Amplitude Converter with Picosecond Resolution" *IEEE Transactions on Instrumentation and Measurement*, Vol.42, No.4, Aug. 1993.
14. Wim van Etten "Distance Determination by Means of Accurate, Periodic Time Interval Measurement" *IEEE Transactions on Instrumentation and Measurement*, Vol.37, No.1, March 1988, pp.155-157.
15. Kiyohide Miyake "Optical Pulsed Ranging: Method for Improving Measurement Accuracy" *Applied Optics*, Vol.15, No.7, July 1976, pp.1684-1685.
16. Joseph W. Goodman, "Comparative Performance of Optical Radar Detection Techniques" *IEEE Transactions on Aerospace and Electronic Systems*, Vol. AES-2, No.5, Sep. 1966, pp.526-535.
17. Pasi Palojarvi, Kari Maatta, Juha Kostamovaara, "Integrated Time-of-Flight Laser Radar" *IEEE Transactions on Instrumentation and Measurement*, Vol.46, No.4, Aug. 1997, pp.996-999.
18. David M Norman, Chester S. Gardner "Satellite Laser Ranging using Pseudonoise Code Modulated Laser Diodes" *Applied Optics*, Vol.27, No.17, Sep. 1988 pp.3650-3655.
19. Gert Stange, Mandyam Srinivasan, Jan Dalczynski "Range Finder Based on Intensity Gradient Measurement" *Applied Optics*, Vol.30, No.13, May 1991, pp.1695-1700.
20. Kannan Krishnaswami, Michael Tilleman, "Off the Line-of-Sight Laser Radar", *Applied Optics*, Vol.37, No.3, Jan 1998, pp.565-572.
21. Hermet.P "Design of a Range Finder for Military Purposes" *Applied Optics*, Vol.11, No.2, Feb. 1972, pp.273-276.
22. Marc Rioux "Laser Range Finder Based on Synchronized Scanners" *Applied Optics*, Vol.23, No.21, Nov. 1984, pp.3837-3844.
23. Kari Maatta, Juha Kostamovaara "A High-precision Time-to-Digital Converter for Pulsed Time-of-Flight Laser Radar Applications" *IEEE Transactions on Instrumentation and Measurement*, Vol.47, No.2, April 1998, pp.521-536.
24. G. Biernson, Lucy R.F, "Requirements of a Coherent Laser Pulse - Doppler Radar" *Proceedings of the IEEE*, Jan. 1963, pp.202-218.

25. Marc Rioux, "Eye-Safe Laser Scanner for Range Imaging", *Applied Optics*, Vol.30, No.16, June 1991, pp.2219-2223.
26. Henshaw.P.D, Sancez.A, Mc sheehy.R.B., "Digital Beam Switch for Agile Beam Laser Radar" *Applied Optics*, Vol.19, No.6, Mar 1980, pp.884 -890.
27. Ikezawa K., Isozaki K., Ueda T. , "Measurement of Absolute Distance Employing a Tunable CW Dye Laser ", *IEEE Transaction on Instrumentation and Measurement*, Vol . 41, No. 1, Feb. 1992, pp. 36-39 .
28. Jozef Kalisz , Ryszard Pelka " Improved Time - Interval Counting Techniques for Laser Ranging Systems ", *IEEE Transaction on Instrumentation and Measurement*, Vol 42, No. 2, April 1993, pp.301- 304 .
29. Tomoteru Kawakami , Michiyuki Endo , Takashi Iwasaki , "Adaptive Multifrequency Modulation Method for an Advanced Laser Range Finder", *IEEE Transaction on Instrumentation and Measurement* , Vol . 43 , No. 6, Dec 1994, pp. 857- 860 .
30. Bridges W.B. , et al. "Coherent Optical Adaptive Techniques" , *Applied Optics*, Vol. 13, No.2, Feb.1974, pp.291-300.
31. Jin Wang, Juha Kostamovaara, "Radiometric Analysis and Simultion of Signal Power Function in a Short Range Laser Radar", *Applied Optics*, Vol. 33 , No.18, 1994, pp.4069-4076.
32. Ghigo F. , et al. "Laser Range Measurements using Non - Gaussian Pulse Shapes", *Applied Optics*, Vol . 15, No. 11, Nov 1976, pp. 2621- 2623.
33. Menyuk N. , Killenger D .K., Menyuk C.R.. "Limitations of Signal Averaging due to Temporal Correlation in Laser Remote- Sensing Measurements", *Applied Optics*, Vol. 21, No. 18, Sep.1982, pp.3377- 3383 .
34. Henshaw P.D., Sanchez A., McSheehy R.B., " Digital Beam Switch for Agile Beam Laser Radar ", *Applied Optics*, Vol . 19 , No. 6, March 1980, pp. 884 - 890.
35. Prasad . K.S.V., "Study of Laser Distance Measurement Techniques", *DIIT Thesis*.
36. Jeffery H. Shapiro , Sun T. Lau, "Turbulence Effects on Coherent Laser Radar Target Statistics", *Applied Optics*, Vol . 21, No.13, July 1982, pp. 2395-2398.
37. F.E. Hoge "Integrated Laser/Radar Satellite Ranging and Tracking System", *Applied Optics*, Vol. 13, No.10, October 1974, pp. 2352-2358.



38. Raimo Ahola, Risto Myllyla "A Time-of-Flight Laser Receiver for Moving Objects", *IEEE Transactions on Instrumentation and Measurement*, Vol. IM-35, No.2, June 1986, pp. 216-221.
39. Michael J. Kavaya, Paul J. M. Suni "Continuous Wave Coherent Laser Radar : Calculation of Measurement Location and Volume", *Applied Optics*, Vol.30, No.18, June 1991, pp. 2634-2642.
40. Kiyodhide Miyake "Correction for Errors in Optical Pulsed range Measurements", *Applied Optics*, Vol. 14, No.3, March 1975, pp. 752-756.
41. William C. Priedhorsky, et al. "Laser Ranging and Mapping with a Photon-Counting Detector", *Applied Optics*, Vol.35, No.3, January 1996, pp.441-451.
42. Malota F., "Pulsed CO<sub>2</sub> laser Heterodyne Radar for Simultaneous Measurements of Range and Velocity", *Applied Optics*, Vol.23, No.19, October 1984, pp.3395-3399.
43. Honeycutt T.E., Otto W.F., "FM-CW Radar Range Measurement with a CO<sub>2</sub> Laser", *IEEE Journal of Quantum Electronics*, Feb 1972, pp.91-92.
44. Taylor M.J., et al, *Applied Optics*, Vol.17, 1978, pp.885-889.
45. Cooke C.R., "Automatic Laser Tracking and Ranging System", *Applied Optics*, Vol.11, No.2, Feb.1972, pp.277-284.
46. Boef A.J.den, "Interferometric Laser Rangefinder using a Frequency Modulated Diode Laser", *Applied Optics*, Vol.26, No.21, Nov.1987, pp.4545-4550.
47. Skolnik M.I., "*Introduction to Radar Systems*", Mc Graw Hill, second edition, 1980, Chapters 6,9,10.
48. Sydenham P.H., "*Handbook of Measure, Science*", Vol.1, John Wiley & Sons, 1982, pp.431-484.
49. Robert Brun, "Gallium-Arsenide Eyesafe Laser Range Finder", *Spie Proceedings*, Vol.1207, 1990, pp.172-181.
50. John M Senior, "*Optical Fiber Communications*", (second edition), Prentice-Hall of India, 1994.
51. G Keiser, "*Optical Fiber Communication*", (second edition), MCGraw Hill, 1991.
52. John Gowar, "*Optical Communication System*", (second edition), PHI, 1993.
53. "System Design and Studies of Fibre Optic Digital Communication Systems", Project Completion Report, ACES, IIT Kanpur, 1984.

**130806**

**130806**

## Date Slip

This book is to be returned on the  
date last stamped.

[illegible]

A130806